

## Discovery and Evaluation of 7-Alkyl-1,5-bis-aryl-pyrazolopyridinones as Highly Potent, Selective, and Orally Efficacious Inhibitors of p38 $\alpha$ Mitogen-Activated Protein Kinase<sup>†</sup>

Liping H. Pettus,<sup>\*,†</sup> Ryan P. Wurz,<sup>†</sup> Shimin Xu,<sup>†</sup> Brad Herberich,<sup>†</sup> Bradley Henkle,<sup>‡</sup> Qiurong Liu,<sup>‡</sup> Helen J. McBride,<sup>‡</sup> Sharon Mu,<sup>‡</sup> Matthew H. Plant,<sup>‡</sup> Christiaan J. M. Saris,<sup>‡</sup> Lisa Sherman,<sup>‡</sup> Lu Min Wong,<sup>‡</sup> Samer Chmait,<sup>§</sup> Matthew R. Lee,<sup>§</sup> Christopher Mohr,<sup>§</sup> Faye Hsieh,<sup>||</sup> and Andrew S. Tasker<sup>†</sup>

<sup>†</sup>Departments of Chemistry Research and Discovery, <sup>‡</sup>Department of Inflammation, <sup>§</sup>Department of Molecular Structure, and <sup>||</sup>Departments of Pharmacokinetics and Drug Metabolism, Amgen Inc., One Amgen Center Drive, Thousand Oaks, California 91320

Received January 22, 2010

The p38 $\alpha$  mitogen-activated protein (MAP) kinase is a central signaling molecule in many proinflammatory pathways, regulating the cellular response to a multitude of external stimuli including heat, ultraviolet radiation, osmotic shock, and a variety of cytokines especially interleukin-1 $\beta$  and tumor necrosis factor  $\alpha$ . Thus, inhibitors of this enzyme are postulated to have significant therapeutic potential for the treatment of rheumatoid arthritis, inflammatory bowel disease, and Crohn's disease, as well as other diseases where aberrant cytokine signaling is the driver of disease. In this communication, we describe a novel class of 7-alkyl-1,5-bis-aryl-pyrazolopyridinone-based p38 $\alpha$  inhibitors. In particular, compound **3f** is highly potent in the enzyme and cell-based assays, selective in an Ambit kinase screen, and efficacious (ED<sub>50</sub>  $\leq$  0.01 mg/kg) in the rat collagen induced arthritis (CIA) model.

### Introduction

p38 $\alpha$  mitogen-activated protein (MAP<sup>α</sup>) kinase is activated by multiple external stimuli including stress and a variety of cytokines, especially tumor necrosis factor  $\alpha$  (TNF $\alpha$ ) and interleukin-1 $\beta$  (IL-1 $\beta$ ).<sup>1</sup> Once activated, it phosphorylates a range of downstream protein substrates, leading to the biosynthesis of TNF $\alpha$  and IL-1 $\beta$ .<sup>2</sup> Excessive production of these cytokines is implicated in many chronic inflammatory diseases, such as rheumatoid arthritis (RA), inflammatory bowel disease, Crohn's disease, and chronic obstructive pulmonary disease (COPD). The proven ability of p38 $\alpha$  MAP kinase to regulate both the production and the activity of these cytokines has prompted many pharmaceutical groups to pursue orally active inhibitors of p38 $\alpha$  for the potential treatment of various inflammatory diseases.<sup>3</sup>

In our previous communications,<sup>4,5</sup> we reported the discovery of 4-methyl-3-phthalazinyl benzamide **1a** (Figure 1) and its bioisostere, 4-methyl-3-phthalazinyl benzoisoxazole **1b**, as potent and selective p38 $\alpha$  inhibitors. Preliminary metabolic studies indicated hydroxylation of the phthalazine ring to be the major metabolic pathway for these compounds. In addition, several lead molecules in the phthalazine series were

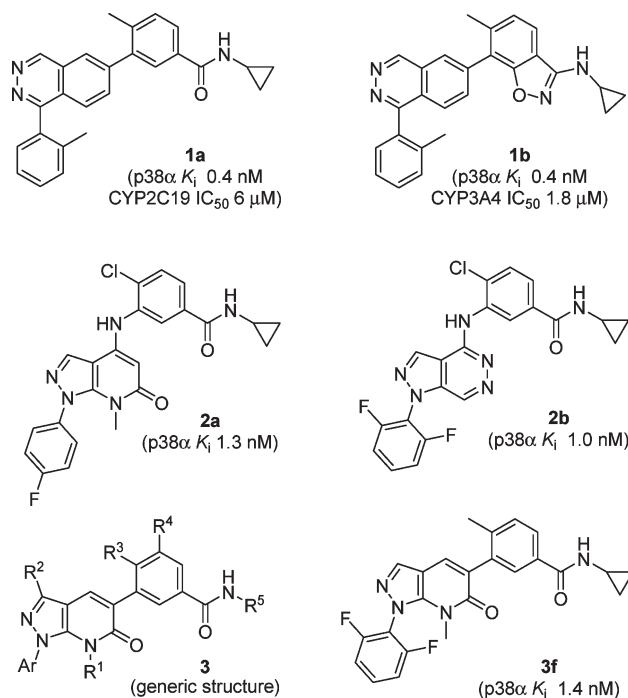


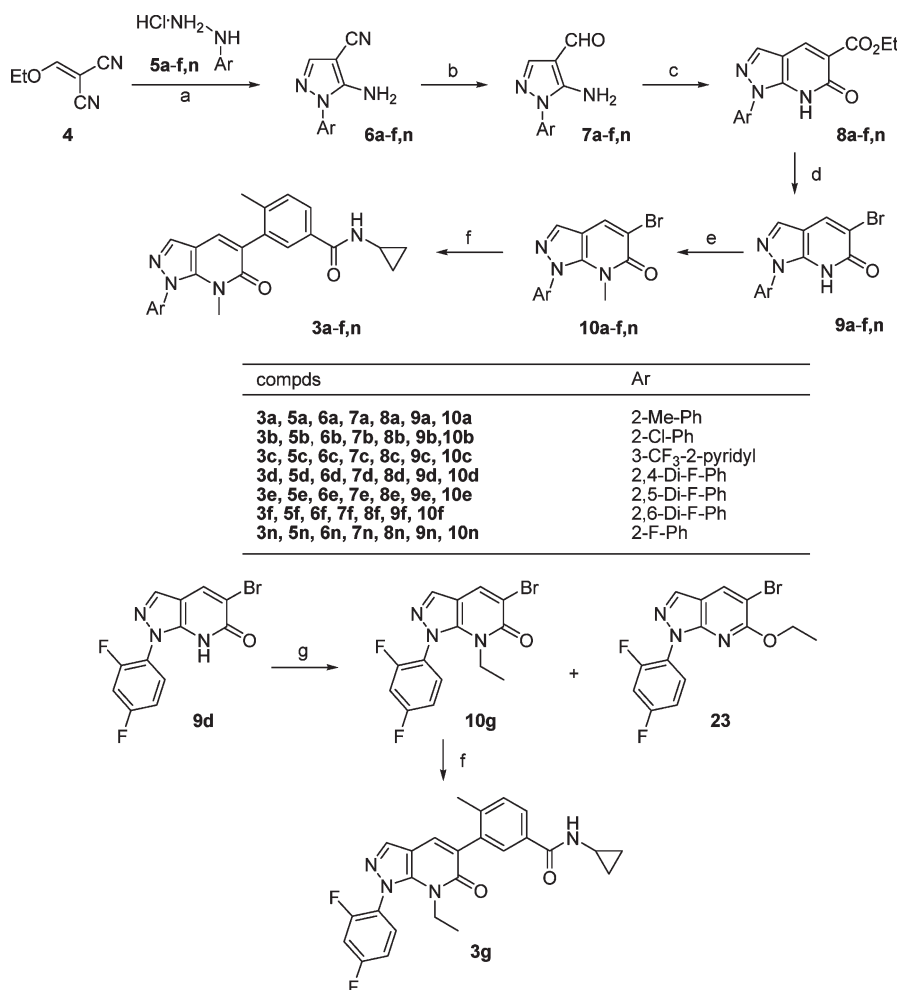
**Figure 1.** Amgen's various p38 $\alpha$  inhibitors.

burdened with moderate-to-strong inhibition of various cytochrome P450 isoforms. To identify novel chemotypes with potentially improved PKDM profiles and reduced brain exposure (for some phthalazine inhibitors, the ratio of concentration in brain/plasma was about one), while maintaining the good potency and selectivity, we sought to replace the phthalazine moiety in compounds **1a** and **1b** with other fused

<sup>†</sup>Atomic coordinates and structure factors for crystal structure of compound **3d** with p38 $\alpha$  can be accessed using PDB code 3LHJ.

\*To whom correspondence should be addressed. Liping Pettus: Tel 805-447-6964; Fax 805-480-1337; e-mail: lpettus@amgen.com.

<sup>α</sup>Abbreviations: AUC, area under the curve; CIA, collagen-induced arthritis; COPD, chronic obstructive pulmonary disease; DFG, Asp-Phe-Gly sequence in ATP binding site; hPXR, human pregnane X receptor; hWB, human whole blood; IL, Interleukin; RA, rheumatoid arthritis; MFI, mean fluorescence intensity; THP1, human acute monocytic leukemia cell line; MAP, mitogen-activated protein; MK2, MAPKAP kinase 2; TNF $\alpha$ , Tumor necrosis factor alpha; hERG, human Ether-a-go-go Related Gene; SAR, structure-activity relationship.

**Scheme 1.** Synthetic Route to the 1,5-Bisaryl-7-Me/Et-pyrazolopyridinones **3a–g,n**<sup>a</sup>

<sup>a</sup> Reagents and conditions: (a) Et<sub>3</sub>N, EtOH, reflux, 1.5 h, quant.; (b) Raney nickel, H<sub>2</sub>, 70% HOAc, 50–80%; (c) diethyl malonate, piperidine, EtOH, reflux, 18 h, >90%; (d) (i) LiOH, CH<sub>3</sub>CN/H<sub>2</sub>O; (ii) NBS, 75–95%; (e) NaH, LiBr, MeI, DME/DMF, 40 °C, 18 h, 50–85%; (f) **11**, Pd<sub>2</sub>(dba)<sub>3</sub>, X-Phos, K<sub>3</sub>PO<sub>4</sub>, dioxane/water, 125 °C, 30 min, microwave, 65–85%; (g) NaH, LiBr, EtI, DME/DMF, 40 °C, 24 h.

bicycles. From these efforts, several fused pyrazole scaffolds were identified. In particular, the structure-activity relationship (SAR) studies of 4-aminoaryl-pyrazolopyridinones (such as **2a**) and 4-aminoaryl-pyrazolopyridazines (such as **2b**) have been the subject of our recent communications.<sup>6</sup> Herein, we report the synthesis and biological evaluation of a novel class of 7-alkyl-1,5-bis-aryl-pyrazolopyridinones (**3**) as p38α inhibitors.<sup>7</sup> The optimized analogue **3f** proved to be potent, selective against other kinases, highly efficacious (ED<sub>50</sub> ≤ 0.01 mg/kg) in the rat CIA model, and devoid of CYP inhibition.

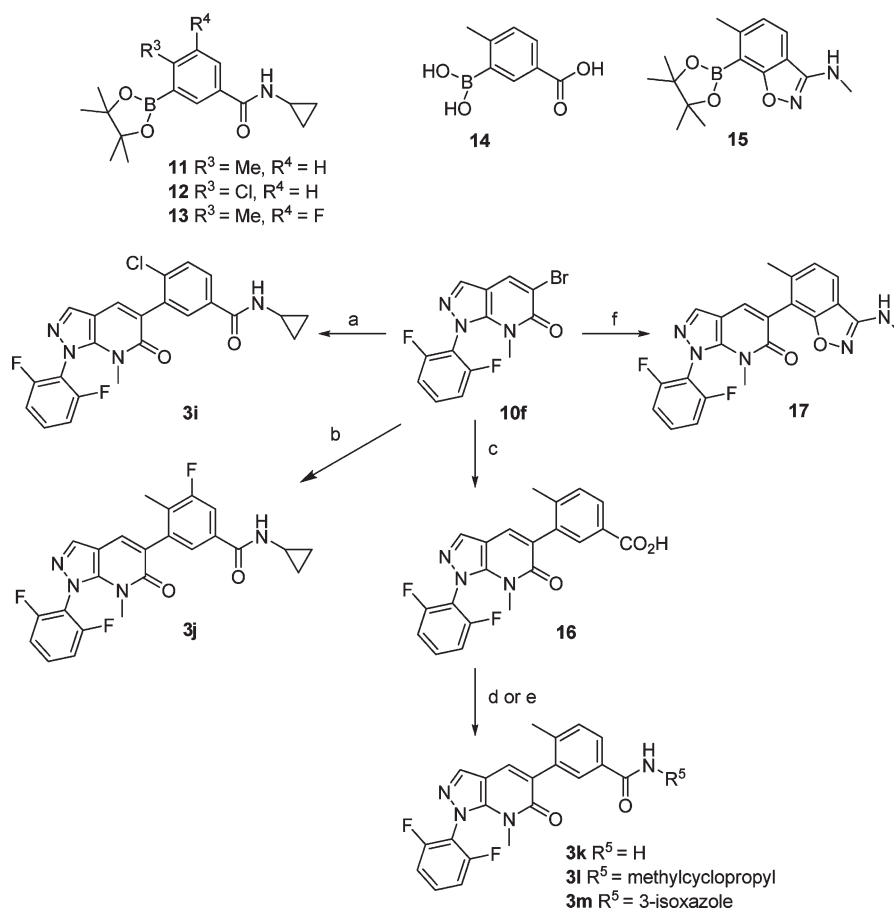
## Chemistry

A general synthetic route to 1,5-bisaryl-7-Me/Et-pyrazolopyridinones **3a–g** and **3n** is shown in Scheme 1. The synthesis commenced with the commercially available aryl hydrazine hydrochloride **5**, which was heated with 2-(ethoxymethylene)-malononitrile (**4**) in ethanol in the presence of triethylamine to furnish 5-amino-1-aryl-pyrazole-4-carbonitrile **6** in quantitative yield. Raney nickel-catalyzed hydrogenation of the carbonitrile in **6** in 70% acetic acid followed by *in situ* hydrolysis of the resulting imine gave aldehyde **7**. Cyclocondensation of **7** with diethylmalonate in the presence of piperidine in boiling ethanol afforded the fused bicyclic ester **8**,<sup>8</sup> which was then

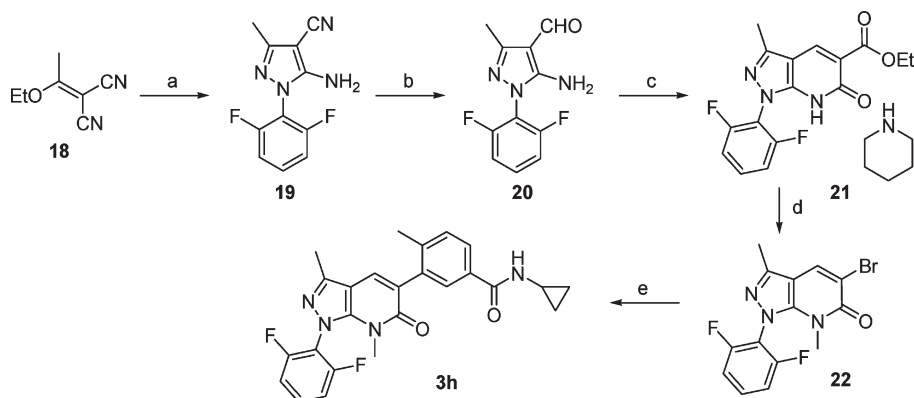
subjected to halodecarboxylation using lithium hydroxide and *N*-bromosuccinimide in aqueous acetonitrile to generate 1-aryl-5-bromo-pyrazolopyridinone **9**.<sup>9</sup> Selective *N*-methylation of **9a–f** and **9n** using NaH/LiBr/MeI in a mixture of DME/DMF (10/1), a procedure that was previously reported by Curran and co-workers to predominantly afford *N*-alkylated pyridinones,<sup>10</sup> produced 1-aryl-5-bromo-7-methyl-pyrazolopyridinones **10a–f** and **10n** in 50–85% yield. Finally, Suzuki coupling of **10a–f** and **10n** with boronic ester **11** (see Scheme 2) afforded benzamides **3a–f** and **3n** in 65–85% yield.

In general, the selective *N*-ethylation of pyridinone **9** was much more difficult to accomplish than the selective *N*-methylation mentioned above. For example, treatment of **9d** with NaH/LiBr/EtI in a mixture of DME/DMF (10/1) gave the *N*-ethyl pyridinone **10g** in only 17% yield, and the ethoxy-pyrazolopyridine **23** in 78% yield. Suzuki coupling of **10g** with boronic ester **11** afforded compound **3g** in 80% yield.

In Scheme 2, the synthesis of 5-aryl-1-(2,6-difluorophenyl)-7-methyl-pyrazolopyridinones was accomplished by either a one-step or two-step procedure. In the one-step fashion, the Suzuki coupling of **10f** with boronic esters **12**, **13**,<sup>3d</sup> and **15**,<sup>5,11</sup> gave benzamides **3i**, **3j**, and benzoisoxazole **17**, respectively. Alternatively, via a two-step procedure, **10f** was coupled with boronic acid **14** to give benzoic acid **16** which served as a

**Scheme 2.** Synthesis of the 5-Aryl-1-(2,6-difluorophenyl)-7-methyl-pyrazolopyridinones (**3i–m**, **17**)<sup>a</sup>

<sup>a</sup> Reagents and conditions: (a) **12**,  $\text{Pd}(\text{PPh}_3)_4$ ,  $\text{Na}_2\text{CO}_3$ , dioxane/water,  $130^\circ\text{C}$ , 25 min, microwave, 44%; (b) **13**,  $\text{Pd}(\text{PPh}_3)_4$ ,  $\text{Na}_2\text{CO}_3$ , dioxane/water,  $130^\circ\text{C}$ , 45 min, microwave, 65%; (c) **14**,  $\text{Pd}(\text{PPh}_3)_4$ ,  $\text{Na}_2\text{CO}_3$ , dioxane/water,  $130^\circ\text{C}$ , 30 min, microwave, 90%; (d) (i) CDI, THF; (ii) 0.5 M  $\text{NH}_3$  in dioxane, 82% for **3k**; (e) (i)  $\text{SOCl}_2$ ; (ii) DMAP,  $\text{EtN}(\text{iPr})_2$ , DCM,  $R^5\text{NH}_2$ , 76% and 35% for **3l** and **3m**, respectively; (f) **15**,  $\text{Pd}(\text{PPh}_3)_4$ ,  $\text{Na}_2\text{CO}_3$ , dioxane/water,  $110^\circ\text{C}$ , 5 h, 63%.

**Scheme 3.** Synthesis of **3h**<sup>a</sup>

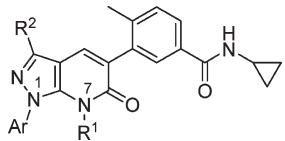
<sup>a</sup> Reagents and conditions: (a) **5f**,  $\text{Et}_3\text{N}$ , EtOH, reflux, 97%; (b) Raney nickel,  $\text{H}_2$ , 70% AcOH, 78%; (c) diethyl malonate, piperidine, EtOH, reflux, 86%; (d) (i) LiOH, MeCN,  $\text{H}_2\text{O}$ ; (ii) NBS; (iii) NaH, LiBr, MeI, DME/DMF, 19% for 3 steps; (e) **11**,  $\text{Pd}(\text{PPh}_3)_4$ ,  $\text{Na}_2\text{CO}_3$ , dioxane/water,  $120^\circ\text{C}$ , microwave, 25 min, 29%.

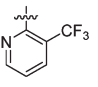
common intermediate for the preparation of benzamides **3k–m**.

As shown in Scheme 3, the synthetic route to 3-Me-pyrazolopyridinone **3h** is analogous to that depicted in Scheme 1 for the 3-des-Me analogue **3f**, with the exception of starting with 2-(1-ethoxyethylidene)malononitrile (**18**) rather than 2-(ethoxymethylene)malononitrile (**4**).

**Results and Discussion**

**In Vitro SAR.** Compounds were evaluated for their ability to inhibit the phosphorylation of activating transcription factor 2 (ATF2) by recombinant human p38 $\alpha$ , as well as LPS-induced TNF $\alpha$  production in THP1 cells. Compounds were also evaluated against TNF $\alpha$ -challenged IL-8 production

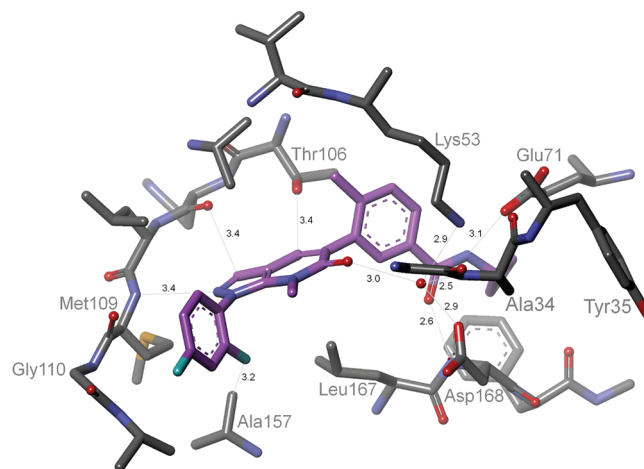
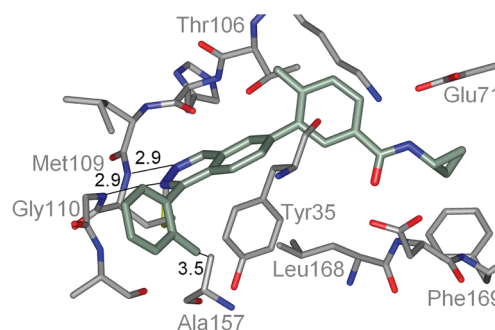
**Table 1.** SAR<sup>a</sup>: Modifications to the Ar, R<sup>1</sup>, and R<sup>2</sup> Groups


compd	Ar	R <sup>1</sup>	R <sup>2</sup>	p38α K <sub>i</sub> (nM)	THP1 LPS/TNFα IC <sub>50</sub> (nM)	hWB TNFα/IL-8 IC <sub>50</sub> (nM)
<b>3a</b>	2-Me-Ph	Me	H	1.9	4.0	12.1
<b>3b</b>	2-Cl-Ph	Me	H	0.9	1.1	8.7
<b>3c</b>		Me	H	2.3	14.4	24
<b>3d</b>	2,4-Di-F-Ph	Me	H	2.3	1.5	3.9
<b>3e</b>	2,5-Di-F-Ph	Me	H	1.9	1.6	3.7
<b>3f</b>	2,6-Di-F-Ph	Me	H	1.4	0.6	1.7
<b>3g</b>	2,4-Di-F-Ph	Et	H	0.6	0.5	2.4
<b>3h</b>	2,6-Di-F-Ph	Me	Me	8.0	2.7	40

<sup>a</sup>The p38α K<sub>i</sub> and IC<sub>50</sub> of cell-based assays are mean values derived from at least three independent dose–response curves. Variability around the mean value was < 50%.

in 50% human whole blood (hWB), an assay that was a more meaningful measurement of inhibitor potency in a physiologically relevant environment due to the presence of serum albumin and other proteins. The TNFα/IL-8 in hWB assay was used as one of the major drivers for compound selection in this program. For advanced compounds, on-mechanism activity was verified by measuring their ability to modulate LPS-driven MAPKAP kinase 2 (MK2) phosphorylation in human whole blood, an event that is currently understood to be mediated solely by p38 MAP kinase.<sup>12</sup>

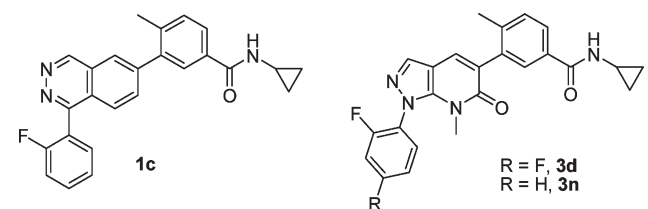
In the generic structure **3** (Figure 1), there were two major sites for SAR investigation: the substitution patterns surrounding the pyrazolopyridinone moiety on the left-hand side of the molecule (Ar, R<sup>1</sup>, and R<sup>2</sup> groups), and the benzamide on the right-hand side of the molecule (R<sup>3</sup>, R<sup>4</sup>, and R<sup>5</sup> groups). The preliminary SAR investigation was focused on the optimization of the N1-Ar group when R<sup>1</sup> = Me and R<sup>2</sup> = H, while conserving the 3-*N*-cyclopropyl-2-methylbenzamide on the right-hand side (Table 1). The *o*-tolyl analogue **3a** (p38α K<sub>i</sub> = 1.9 nM, TNFα/IL-8 IC<sub>50</sub> = 12.1 nM), the first compound made in this series, was about 5-fold weaker than its phthalazinyl counterpart **1a** (Figure 1) in both enzyme and cell-based assays. For the other two *ortho*-substituted analogues, **3b** (Ar = 2-Cl-Ph) was comparable to **3a** in terms of potency in the TNFα/IL-8 assay, while **3c** (Ar = 3-CF<sub>3</sub>-2-pyridyl) was 2-fold weaker than **3a**. Although the difluorinated analogues, **3d** (2,4-Di-F-Ph), **3e** (2,5-Di-F-Ph), and **3f** (2,6-Di-F-Ph), were similar to **3a** in p38α activity (K<sub>i</sub> in the range 1.4–2.3 nM), they were more potent than **3a** in the cell-based assays, with almost no shift between enzyme and hWB potency.

**Figure 2.** X-ray crystal structure of compound **3d** bound in the ATP binding site of unphosphorylated p38α. Bond distances are given in angstroms. For the inhibitor, C: purple; F: cyan; N: blue; O: red.**Figure 3.** X-ray crystal structure of compound **1a** bound in the ATP binding site of unphosphorylated p38α. PDB code 3DS6. Bond distances are given in angstroms. For the inhibitor, C: green; N: Blue; O: Red.

Increasing the size of the N7-R<sup>1</sup> group from Me to Et generally improved the p38α potency, for example, **3d** (K<sub>i</sub> 2.3 nM) versus **3g** (K<sub>i</sub> 0.6 nM). However, the N7-Et analogue **3g** was not advanced further due to its strong CYP3A4 inhibition (IC<sub>50</sub> = 1.6 μM) and elevated human pregnane X receptor (hPXR) activity.<sup>13</sup> In comparison, neither CYP inhibition nor hPXR trans-activation was an issue for any of the N7-Me analogues in Table 1. Finally, in the last row of Table 1, the C3-Me analog **3h** (p38α K<sub>i</sub> = 8.0 nM) was nearly 4-fold weaker than **3f** in both p38α and THP1 assays, and 20-fold weaker than **3f** in the TNFα/IL-8 assay.

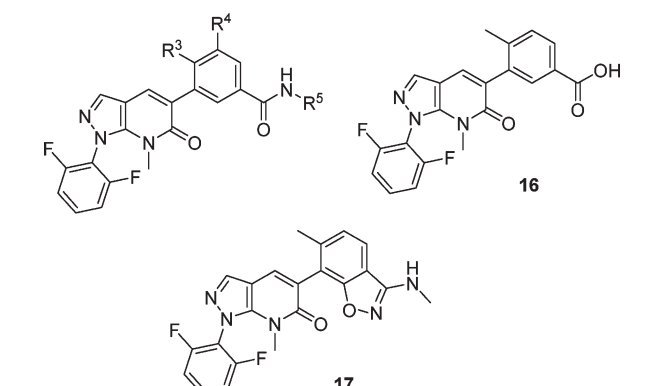
A crystal structure of the unphosphorylated p38α/**3d** complex<sup>14</sup> (Figure 2) reveals that the binding of **3d** with the protein includes three H-bond interactions: the cyclopropyl amide carbonyl oxygen with the backbone NH of Asp168; the cyclopropyl amide NH with the carboxylate of Glu71 located on the C-helix; and the pyrazolo nitrogen (N2) with the linker Met109. The CH<sub>3</sub>-group in the benzamide moiety occupies the Thr106 “gatekeeper pocket”. The cyclopropyl group is nested against Phe169 that resides DFG-in.<sup>15</sup> In stark contrast to the phthalazine-based system (Figure 3, cocrystal of **1a** and p38α),<sup>4</sup> the *N*-methylpyridinone subunit in **3d** forces a reorganization of the P-loop; a bound water molecule bridges the pyridinone carbonyl to the carboxylate of Asp168, the ammonium terminus of Lys53, and the backbone NH of Ala34 on the reoriented P-loop; and Tyr35 no longer engages the inhibitor as it does with the



**Table 2.** Binding Constant ( $K_d$ ) Values of Phthalazine **1c** and Pyrazolopyridinones **3d** and **3n** towards p38 $\alpha$ , Kdr, Lck, and cKit<sup>a</sup>


compd	p38 $\alpha$ (nM)	Kdr (nM)	Lck (nM)	cKit (nM)
<b>1c</b>	0.05	320	530	2.4
<b>3d</b>	0.31	40 000	40 000	13 000
<b>3n</b>	0.18	40 000	40 000	1700

<sup>a</sup>  $K_d$  (an average of two values) measurements were performed by Ambit Bioscience.

**Table 3.** SAR<sup>a</sup>: Benzamides (Modifications to the R<sup>3</sup>, R<sup>4</sup>, and R<sup>5</sup> Groups), Benzoic Acid (**16**) and Benzoisoxazole (**17**)


compd	R <sup>3</sup>	R <sup>4</sup>	R <sup>5</sup>	p38 $\alpha$ $K_i$ (nM)	THP1 LPS/TNF $\alpha$ IC <sub>50</sub> (nM)	hWB TNF $\alpha$ /IL-8 IC <sub>50</sub> (nM)
<b>3f</b>	Me	H		1.4	0.6	1.7
<b>3i</b>	Cl	H		1.1	0.9	4.4
<b>3j</b>	Me	F		0.8	0.4	1.7
<b>3k</b>	Me	H	H	1.5	3.9	6.4
<b>3l</b>	Me	H		1.7	2.7	11
<b>3m</b>	Me	H		1.0	0.3	1.5
<b>16</b>	Me	H	--	458	631	>2500
<b>17</b>	Me	H	--	2.0	1.2	5.4

<sup>a</sup> The p38 $\alpha$   $K_i$  and IC<sub>50</sub> of cell-based assays are mean values derived from at least three independent dose–response curves. Variability around the mean value was < 50%.

phthalazine. The 2,4-difluorophenyl group is oriented perpendicular to the pyrazolopyridinone, a feature driven by the adjacent *N*-methyl group, and nests in a hydrophobic pocket formed by the linker strand, Leu167 from the activation loop

**Table 4.** PK Profiles of Lead Compounds in Sprague-Dawley Rats Following Intravenous (IV) and Oral (PO) Dose<sup>a</sup>

compd	IV (2.0 mg/kg in DMSO)			PO (2 mg/kg) <sup>b</sup>	
	CL (mL/h/kg)	$V_{dss}$ (mL/kg)	$t_{1/2}$ (h)	AUC <sub>(0-∞)</sub> (ng·h/mL)	F (%)
<b>3d</b>	173	1690	7.7	5124	73
<b>3e</b>	247	955	2.2	782	10
<b>3f</b>	220	837	2.7	3990	43
<b>3i</b>	165	1466	6.3	8857	73
<b>3k</b>	312	1105	2.4	2393	37
<b>17</b>	1055	1888	3.5	515	27

<sup>a</sup> Values are an average of three rats. <sup>b</sup> Vehicle = 1% Pluronic F68, 1% HPMC, 15% hydroxypropyl beta cyclodextrin and 83% water.

and Ala157 on the floor of the ATP binding site. An alanine residue at this location is present in only seven proteins within the kinome;<sup>16</sup> hence, exploiting this feature with a rigid inhibitor provides a superior selectivity profile for pyrazolopyridinones **3d** and **3n** relative to that observed with phthalazine **1c**<sup>4b</sup> (Table 2).<sup>17</sup> In contrast to the phthalazines, the pyrazolopyridinones do not cause the backbone Gly110 to flip, a binding motif that has been shown to contribute to kinase selectivity.<sup>4a,5</sup> However, because the pyrazolopyridinones explore both features of Ala157 and Thr106 (a relatively small gatekeeper) more effectively, they end up being more selective p38 $\alpha$  inhibitors than the phthalazines, such as against Kdr, LCK, and cKit. This phenomenon of exquisite kinase selectivity is also observed in two other fused pyrazole scaffolds, the 4-aminoaryl-pyrazolopyridinones (such as **2a**)<sup>6a</sup> and 4-aminoaryl-pyrazolopyridazines (such as **2b**).<sup>6b</sup>

We next examined the SAR of the benzamide portion (R<sup>3</sup>, R<sup>4</sup>, and R<sup>5</sup>) while conserving the 1-(2,6-difluorophenyl)-7-methyl-pyrazolopyridinone moiety (Table 3). The three *N*-cyclopropyl benzamides, **3f**, **3i**, and **3j**, had comparable potency in enzyme ( $K_i$  0.8–1.4 nM), THP1 (IC<sub>50</sub> 0.4–0.9 nM), and hWB (IC<sub>50</sub> 1.7–4.4 nM) assays. Replacement of the cyclopropyl amide in **3f** with a smaller primary amide (**3k**) or a bulkier 1-methylcyclopropyl amide (**3l**) resulted in nearly equal p38 $\alpha$  potency ( $K_i$  1.5–1.7 nM), but reduced hWB potency (IC<sub>50</sub> = 6.4 and 11 nM for **3k** and **3l**, respectively). The isoxazole derived amide **3m** was equally potent to **3f** in all 3 assays, which demonstrated that small heterocycles could be good replacements for the cyclopropyl group. However, compounds **3j** and **3m** were not further pursued due to highly elevated hPXR level observed with these compounds.<sup>13,18</sup> The carboxylic acid **16**, a major metabolite of amide **3f** in rats, had weak inhibitory activity on p38 $\alpha$  ( $K_i$  = 458 nM) and almost no measurable activity in the hWB TNF $\alpha$ -IL8 assay (IC<sub>50</sub> > 2.5  $\mu$ M). Lastly, the benzoisoxazole **17**, an amide bioisostere, also demonstrated good potency in the hWB assay (IC<sub>50</sub> = 5.4 nM).

Several potent compounds (TNF $\alpha$ /IL-8 IC<sub>50</sub> < 7 nM) were selected for assessment of their pharmacokinetic (PK) profiles in male Sprague–Dawley rats (Table 4). With the exception of benzoisoxazole **17**, all compounds showed low clearance (CL). Since p38 inhibitors with high brain exposure have been reported to cause central nervous system toxicity in preclinical toxicology studies,<sup>3f,19</sup> one of the goals for this program was to design inhibitors with limited potential to cross the blood brain barrier. Gratifyingly, the pyrazolopyridinone benzamides in Table 4 all showed low brain exposure, with the ratio of concentration in brain/plasma being < 0.08. This event is likely driven by the higher PSA and lower cLogP of the pyrazolopyridinone

benzamides than that of the phthalazine benzamides. For example, the PSA and cLogP for pyrazolopyridinone amide **3f** are 70.0 and 3.5, respectively; while the PSA and cLogP for phthalazine amide **1a** are 54.8 and 4.3, respectively.<sup>20</sup> Furthermore, compounds **3d**, **3f**, and **3i**, which displayed exceptional oral exposure (AUC) and good bioavailability (*F*%) upon oral dosing at 2 mg/kg, were advanced for further testing.

For a proximal readout of the on-target effects of these inhibitors, we measured the inhibition of LPS-induced MAPKAP kinase 2 (MK2) phosphorylation in whole cells. To the best of our knowledge, this is the first time a pMK2 assay is reported in a SAR article; thus, a brief description of the assay is warranted. Human peripheral blood was incubated with various concentrations of inhibitor in the presence or absence of LPS (1  $\mu$ g/mL), then fixed and permeabilized for staining of intracellular proteins. Phosphorylated MK2 was detected with fluorochrome-conjugated anti-pMK2 antibody, and levels of phosphorylation were determined by flow cytometry (FACS Calibur, BD, San Jose, CA) and presented as mean fluorescence intensity (MFI) of labeled cells. Results were expressed as POC (percentage of control) of MFI where LPS-treated blood in the absence of compound was used as 100% control. Data were analyzed by GraphPad Prism 4.01 (GraphPad Software Inc. San Diego, CA). Using **3f**

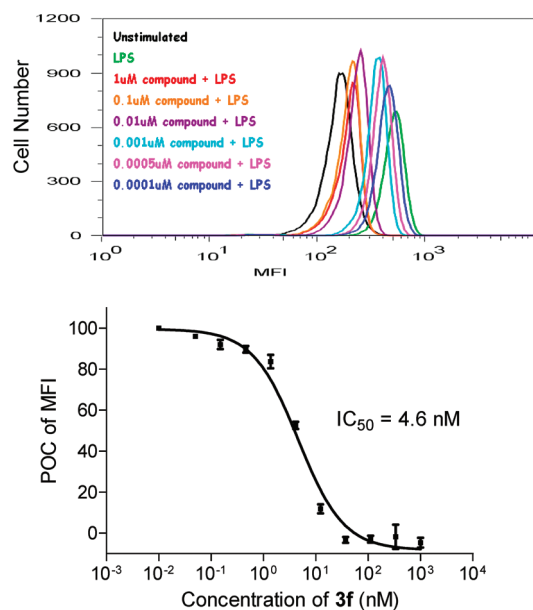


**Figure 4.** Inhibition of LPS-induced MK2 phosphorylation in 50% hWB by **3f**. Human peripheral blood was incubated with various concentrations of **3f** in the presence or absence of 1  $\mu$ g/mL LPS. MK2 phosphorylation was measured by MFI as presented in the top figure. Results were expressed as POC of MFI where unstimulated samples served as background, and LPS-stimulated no-compound treated samples as 100% (bottom figure). Duplicates were run for each concentration point. This is a representative of 5 experiments.

**Table 5.** Additional Profiling on the Lead Compounds: Inhibition of LPS-Induced MK2 Phosphorylation in 50% hWB, Plasma Protein Binding and Cell Permeability

compd	pMK2		protein binding (%) <sup>b</sup>		Caco-2 <sup>c</sup>	
	IC <sub>50</sub> (nM)	<i>n</i> <sup>a</sup>	human	rat	<i>P</i> <sub>app</sub> A>B (cm/s)	<i>P</i> <sub>app</sub> B>A (cm/s)
<b>3d</b>	5.7 $\pm$ 1.0	5	93.0	92.5	20 $\times$ 10 <sup>-6</sup>	29 $\times$ 10 <sup>-6</sup>
<b>3f</b>	4.3 $\pm$ 0.5	5	92.1	91.3	27 $\times$ 10 <sup>-6</sup>	27 $\times$ 10 <sup>-6</sup>
<b>3i</b>	7.0 $\pm$ 1.6	4	96.2	96.8	25 $\times$ 10 <sup>-6</sup>	18 $\times$ 10 <sup>-6</sup>

<sup>a</sup> Number of replicates. <sup>b</sup> Determined by the ultrafiltration methods (*n* = 1). <sup>c</sup> Human colon carcinoma cell line (Caco-2); apparent permeability coefficient (*P*<sub>app</sub>); results from single assay (*n* = 1).

as an example, Figure 4 shows the data that is presented in graphs. In Table 5, the single digit nM potency (IC<sub>50</sub>) of the pMK2 inhibition of the three lead compounds, **3d**, **3f**, and **3i**, was consistent with their single digit nanomolar potency in the cytokine production inhibition (Table 1 and Table 3). Again, there was a minimal shift in potency from the enzyme assay to the LPS-pMK2 in 50% hWB assay, which could be attributed to the fact that these inhibitors were not highly plasma protein bound and were quite permeable (Table 5).

To evaluate kinase selectivity, **3f** was tested at 1  $\mu$ M against a panel of 317 kinases using the Ambit Biosciences Kinomescan platform.<sup>21</sup> Only 4 kinases, namely, p38 $\alpha$ , p38 $\beta$ , PDGFRA, and RAF1, have POC < 50%. Subsequently, *K*<sub>d</sub> determinations were performed by Ambit Bioscience and the data is as follows: p38 $\alpha$  (0.25 nM), p38 $\beta$  (0.67 nM), PDGFRA (1100 nM), and RAF1 (1100 nM). As with other reported p38 $\alpha$  inhibitors,<sup>3f,22</sup> **3f** was selective against p38 $\gamma$  (*K*<sub>i</sub> = 3500 nM) and p38 $\delta$  (*K*<sub>i</sub> = 2100 nM) isoforms, but not against p38 $\beta$  (*K*<sub>i</sub> = 2.5 nM). In a broader selectivity screen against a variety of G-protein coupled receptors and ion channels, **3f** did not exhibit any off-target interactions when tested at 10  $\mu$ M concentration. Furthermore, it yielded an IC<sub>50</sub> of 36  $\mu$ M for blockade of the hERG cardiac channel determined by manual electrophysiology. It was negative in both Ames and Micronucleus (MN) assays. Additional profiling of **3f** showed minimal inhibition of five of the principal cytochrome P450 isoforms (1A2, 2C9, 2C19, 2D6, and 3A4, IC<sub>50</sub> > 25  $\mu$ M);<sup>23</sup> and at a concentration of 25  $\mu$ M, there was no induction of CYP1A2, 2B6, 2C9, and 3A4.<sup>24</sup> It had low potential in hPXR transactivation (5% and 13% of positive control when tested at 2 and 10  $\mu$ M, respectively). Although **3d** and **3i** showed profiles similar to that of **3f** when screened in the above-mentioned selectivity, safety, and metabolic panels, ultimately only **3f** was advanced for further testing based on its better solubility and more linear exposure in rats (data not shown) than its two close analogues.

### In Vivo Pharmacology

The rat collagen induced arthritis (CIA) model was chosen as the preclinical disease model for RA.<sup>25</sup> Compound **3f** was administered orally at 0.01, 0.03, 0.1, 0.3, and 1.0 mg/kg once daily to rats, beginning on day 10 through day 17 following immunization. As shown in Figure 5, **3f** inhibited paw swelling in the CIA model in a dose-dependent manner with an ED<sub>50</sub> of  $\leq$ 0.01 mg/kg, corresponding to an exposure of AUC (0–24 h) = 180 nM h, with an interpolated *C*<sub>max</sub> and *C*<sub>24 h</sub> of 11 nM and 4.4 nM, respectively. On-target activity was verified by the measurement of MK2 phosphorylation in the ankles of two rats chosen randomly from the studied group. Compound **3f** showed an ED<sub>50</sub> of  $\leq$ 0.01 mg/kg for the inhibition of MK2 phosphorylation, which correlated well with the efficacy for inhibition of paw swelling.

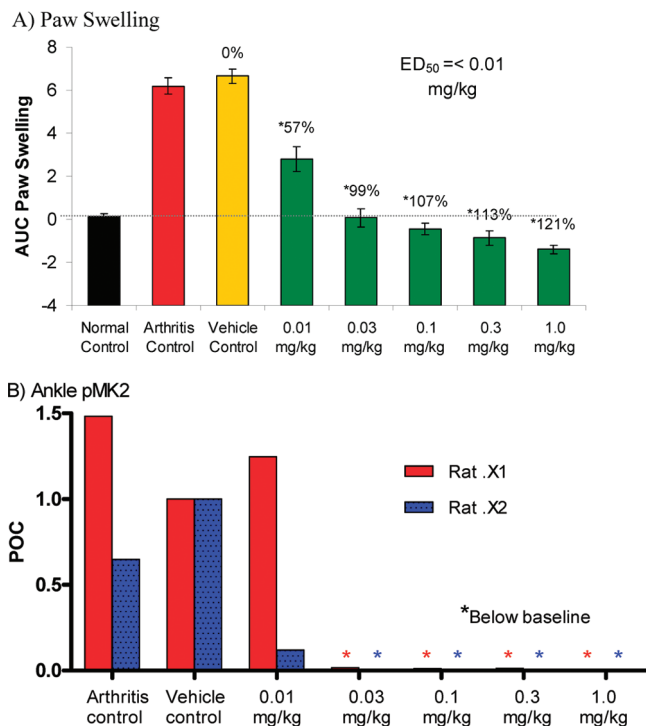


**Figure 5.** Effect of **3f** on CIA in Lewis Rats. Arthritis was induced by intradermal injection of Porcine Type II collagen emulsified 1:1 in Incomplete Freund's Adjuvant (IFA). Animals were assigned to treatment groups at disease onset (study day 0), which occurred 10–12 days following immunization. Compound **3f** or vehicle (15% HPBCD, 1% HPMC, 1% Pluronic F68, pH 2.2) was administered orally once a day for 7 days. (A) Paw diameter was measured daily from day 0 through day 7. Area under the paw swelling curve (AUC) was calculated and used to determine percent inhibition of inflammation compared with vehicle controls. Data points represent mean  $\pm$  ste ( $n = 8$  rats/group). \*  $p \leq 0.05$  vs vehicle control. (B) Rat ankles ( $n = 2$  per group) were frozen immediately after decapitation. The ankles were later pulverized, and lysed with lysis buffer. Fifteen micrograms of protein lysate was loaded in each lane for Western analysis. The blot was probed with phosphor-MK2 antibody. MK2 signal intensities were quantitated using Nonlinear's Phoretix 1D software version 2003 02 and normalized to the Akt loading control and expressed them as POC (vehicle + arthritis as 100%).

## Conclusions

A structurally novel pyrazolopyridinone series has been discovered as p38 $\alpha$  MAP kinase inhibitors. An X-ray crystal structure of p38 $\alpha$ /**3d** indicated that the N1-Ar group engaged in van der Waals contact with an uncommon floor residue, Ala157, thus providing a structure-based approach for achieving selectivity over other kinases. Through SAR studies, several analogues with single digit nanomolar potency in both enzyme and cell-based assays were identified. In particular, **3f** was highly selective against other kinases and devoid of CYP inhibition and induction. Furthermore, with a desirable pharmacokinetic profile, **3f** was highly efficacious (ED<sub>50</sub>  $\leq$  0.01 mg/kg) in the rat CIA model.

## Experimental Section

**Chemistry.** All reagents and solvents were obtained from commercial suppliers and used without further purification. All reactions were carried out under an inert atmosphere of nitrogen unless otherwise noted. All microwave-assisted reactions were conducted with a Smith synthesizer from Personal Chemistry, Uppsala, Sweden. Silica gel chromatography was performed using either glass columns packed with silica gel

(200–400 mesh, Aldrich Chemical) or prepacked silica gel cartridges (Biotage and ISCO). <sup>1</sup>H NMR spectra were obtained on Bruker DRX 400 (400 MHz) spectrometer and reported as ppm downfield from tetramethylsilane. All tested compounds were purified to >95% purity as determined by HPLC. HPLC analysis was obtained on Agilent 1100, using one or two of the following three methods. HPLC Method A (3.6 min LC-MS Run): Zorbax analytical C18 column (50  $\times$  3 mm, 3.5  $\mu$ m, 40  $^{\circ}$ C); mobile phase: A = 0.1% TFA in Water, B = 0.1% TFA in acetonitrile; gradient: 0.0–3.6 min, 5–95% B; flow rate = 1.5 mL/min;  $\lambda$  = 254 nm; 0 min post time; 1.0  $\mu$ L injection. HPLC Method B (10 min LC-MS Run): YMC ODS-AM (100  $\times$  2.1 mm, 5  $\mu$ m, 40  $^{\circ}$ C); mobile phase: A = 0.1% HCOOH in Water, B = 0.1% HCOOH in acetonitrile; gradient: 0.0–0.5 min, 10% B; 0.5–7.0 min, 10–100% B; 7.0–10 min, 100% B; flow rate = 0.5 mL/min;  $\lambda$  = 254 nm; 1.5 min post time; 3.0  $\mu$ L injection. HPLC Method C (5 min LC-MS Run): Phenomenex Synergi MAX-RP (50  $\times$  2.0 mm, 4.0  $\mu$ m, 40  $^{\circ}$ C); mobile phase: A = 0.1% TFA in Water, B = 0.1% TFA in acetonitrile; gradient: 0.0–0.2 min, 10% B, 0.2–3.0 min, 10–100% B, 3.0–4.5 min, 100% B, 4.5–5.0 min, 100–10% B; flow rate = 0.8 mL/min;  $\lambda$  = 254 nm; 1.5 min post time; 3.0  $\mu$ L injection. Low-resolution mass spectral (MS) data were determined on a Perkin-Elmer-SCIEX API 165 mass spectrometer using ES ionization modes (positive or negative).

**5-Amino-1-(2,6-difluorophenyl)-1H-pyrazole-4-carbonitrile (6f).** To a solution of 1-(2,6-difluorophenyl)hydrazine hydrochloride (12.38 g, 68.56 mmol) in anhydrous ethanol (70 mL) at RT was added 2-(ethoxymethylene)malononitrile (8.79 g, 71.98 mmol) followed by triethylamine (10.01 mL, 71.98 mmol). The reaction mixture was stirred at RT for 10 min, then heated at 75  $^{\circ}$ C in an oil bath for 1.5 h. The contents were cooled to RT and solvents removed under reduced pressure. The remaining brown solid was stirred in 50 mL of water and 150 mL of EtOAc. The aqueous layer was separated and extracted with 150 mL of EtOAc. The combined EtOAc solution was washed with 50 mL of brine, dried, and concentrated. The remaining residue was stirred in 50 mL of hexanes, and the insoluble material was filtered through a fritted funnel to give 5-amino-1-(2,6-difluorophenyl)-1H-pyrazole-4-carbonitrile (14.97 g, 99% yield) as a brown solid, which was used in the next step without further purification. <sup>1</sup>H NMR (DMSO-*d*<sub>6</sub>):  $\delta$  7.84 (s, 1 H), 7.68 (m, 1 H), 7.36 (m, 2 H), 6.96 (br., 2 H). MS (ESI, pos. ion)  $m/z$ : 221.1 (M+1). HPLC (Method A): retention time 1.37 min.

A similar procedure was used to prepare compounds **6a–e** and **6n**.

**5-Amino-1-*o*-tolyl-1H-pyrazole-4-carbonitrile (6a).** <sup>1</sup>H NMR (DMSO-*d*<sub>6</sub>):  $\delta$  7.75 (s, 1 H), 7.31–7.47 (m, 3 H), 7.24–7.30 (m, 1 H), 6.44 (s, 2 H), 2.04 (s, 3 H). MS (ESI, pos.ion)  $m/z$ : 199.0 (M+1). HPLC (Method B): retention time 4.16 min.

**5-Amino-1-(2-chlorophenyl)-1H-pyrazole-4-carbonitrile (6b).** <sup>1</sup>H NMR (DMSO-*d*<sub>6</sub>):  $\delta$  7.77 (s, 1 H), 7.67 (d,  $J$  = 7.5 Hz, 1 H), 7.58 (m, 1 H), 7.51 (m, 2 H), 6.67 (br, 2 H). MS (ESI, pos.ion)  $m/z$ : 219.0 (M+1). HPLC (Method B): retention time 4.21 min.

**5-Amino-1-(3-(trifluoromethyl)pyridin-2-yl)-1H-pyrazole-4-carbonitrile (6c).** <sup>1</sup>H NMR (CDCl<sub>3</sub>):  $\delta$  8.66 (d,  $J$  = 4.0 Hz, 1 H), 8.28 (d,  $J$  = 8.0 Hz, 1 H), 7.67 (s, 1 H), 7.50 (dd,  $J$  = 7.8, 4.8 Hz, 1 H), 5.79 (br., 2 H). MS (ESI, pos.ion)  $m/z$ : 254.0 (M+1). HPLC (Method A): retention time 1.42 min.

**5-Amino-1-(2,4-difluorophenyl)-1H-pyrazole-4-carbonitrile (6d).** <sup>1</sup>H NMR (DMSO-*d*<sub>6</sub>):  $\delta$  7.79 (s, 1 H), 7.49–7.64 (m, 2 H), 7.26 (t,  $J$  = 8.5 Hz, 1 H), 6.80 (s, 2 H). MS (ESI, pos.ion)  $m/z$ : 221.0 (M+1). HPLC (Method B): retention time 4.01 min.

**5-Amino-1-(2,5-difluorophenyl)-1H-pyrazole-4-carbonitrile (6e).** <sup>1</sup>H NMR (CDCl<sub>3</sub>):  $\delta$  7.74 (s, 1 H), 7.36–7.26 (m, 2 H), 7.20 (m, 1 H), 4.55 (br, 2 H). MS (ESI, pos.ion)  $m/z$ : 221.1 (M+1). HPLC (Method A): retention time 1.42 min.

**5-Amino-1-(2-fluorophenyl)-1H-pyrazole-4-carbonitrile (6n).** <sup>1</sup>H NMR (DMSO-*d*<sub>6</sub>):  $\delta$  7.79 (s, 1 H), 7.56–7.48 (m, 3 H), 7.67 (s, 1 H), 7.44 (m, 1 H), 6.67 (br., 2 H). MS (ESI, pos.ion)  $m/z$ : 202.9 (M+1). HPLC (Method B): retention time 3.03 min.



**5-Amino-1-(2,6-difluorophenyl)-1H-pyrazole-4-carbaldehyde (7f).** To a solution of 5-amino-1-(2,6-difluorophenyl)-1H-pyrazole-4-carbonitrile (**6f**) (50.02 g, 227 mmol) in 70% acetic acid (250 mL) was added Raney nickel (Aldrich, active catalyst slurry in water, 10 g), and the contents were purged with hydrogen (30 psi) and backfilled with argon. This was done twice, and the contents were stirred vigorously under a positive pressure of hydrogen (30 psi) for 24 h. The reaction mixture was filtered through a pad of Celite to remove nickel and the filter bed washed with 2 × 30 mL of 70% acetic acid. The filtrate was concentrated under reduced pressure to remove most of the solvent. To the remaining residue at 0 °C was added water (90 mL) dropwise, and the resulting mixture was stirred at RT for 1 h. The precipitated brown solid was filtered through a fritted funnel, washed with water (2 × 30 mL), and collected. It was dried in a vacuum oven at 45 °C for 18 h to afford the title compound (40.3 g, 79%) as a tan crystalline solid. <sup>1</sup>H NMR (CDCl<sub>3</sub>): δ 9.73 (s, 1 H), 7.89 (s, 1 H), 7.51 (m, 1 H), 7.14 (m, 2 H), 5.65 (br, 2 H). MS (ESI, pos.ion) *m/z*: 224.0 (M+1). HPLC (Method A): retention time 1.22 min.

A similar procedure was used to prepare compounds **7a–e** and **7n**.

**5-Amino-1-*o*-tolyl-1H-pyrazole-4-carbaldehyde (7a).** <sup>1</sup>H NMR (CDCl<sub>3</sub>): δ 9.73 (s, 1 H), 7.81 (s, 1 H), 7.28–7.46 (m, 4 H), 5.46 (br, 2 H), 2.17 (s, 3 H). MS (ESI, pos.ion) *m/z*: 202.0 (M+1). HPLC (Method A): retention time 1.27 min.

**5-Amino-1-(2-chlorophenyl)-1H-pyrazole-4-carbaldehyde (7b).** <sup>1</sup>H NMR (CDCl<sub>3</sub>): δ 9.73 (s, 1 H), 7.84 (s, 1 H), 7.560 (m, 1 H), 7.47 (m, 3 H), 5.59 (br, 2 H). MS (ESI, pos.ion) *m/z*: 222.0 (M+1). HPLC (Method C): retention time 2.06 min.

**5-Amino-1-(3-(trifluoromethyl)pyridin-2-yl)-1H-pyrazole-4-carbaldehyde (7c).** <sup>1</sup>H NMR (CDCl<sub>3</sub>): δ 9.74 (s, 1 H), 8.61–8.69 (m, 1 H), 8.23–8.29 (m, 1 H), 7.82 (s, 1 H), 7.46 (dd, *J* = 7.8, 4.8 Hz, 1 H), 7.08 (br., 2 H). MS (ESI, pos.ion) *m/z*: 257.0 (M+1). HPLC (Method C): retention time 1.37 min.

**5-Amino-1-(2,4-difluorophenyl)-1H-pyrazole-4-carbaldehyde (7d).** <sup>1</sup>H NMR (CDCl<sub>3</sub>): δ 9.73 (s, 1 H), 7.84 (s, 1 H), 7.53 (td, *J* = 8.8, 6.0 Hz, 1 H), 7.01–7.13 (m, 2 H), 5.69 (br, 2 H). MS (ESI, pos.ion) *m/z*: 224.0 (M+1). HPLC (Method B): retention time 3.44 min.

**5-Amino-1-(2,5-difluorophenyl)-1H-pyrazole-4-carbaldehyde (7e).** <sup>1</sup>H NMR (CDCl<sub>3</sub>): δ 9.75 (s, 1 H), 7.89 (s, 1 H), 7.41–7.21 (m, 3 H), 5.70 (br, 2 H). MS (ESI, pos.ion) *m/z*: 224.0 (M+1). HPLC (Method C): retention time 2.08 min.

**5-Amino-1-(2-fluorophenyl)-1H-pyrazole-4-carbaldehyde (7n).** <sup>1</sup>H NMR (CDCl<sub>3</sub>): δ 9.73 (s, 1 H), 7.84 (s, 1 H), 7.54 (m, 2 H), 7.33 (m, 2 H), 5.73 (br, 2 H). MS (ESI, pos.ion) *m/z*: 206.0 (M+1).

**Ethyl 1-(2,6-difluorophenyl)-6-oxo-6,7-dihydro-1H-pyrazolo[3,4-*b*]pyridine-5-carboxylate (8f).** In a 500 mL round-bottomed flask was weighed 5-amino-1-(2,6-difluorophenyl)-1H-pyrazole-4-carbaldehyde (**7f**) (7.77 g, 35 mmol) followed by ethanol (100 mL). The solution was treated with diethyl malonate (11 mL, 70 mmol) and piperidine (3.4 mL, 35 mmol) and heated at 75 °C in an oil bath overnight. The reaction mixture was concentrated under reduced pressure and the brown residue was treated with 200 mL of a 1:1 solution of EtOAc/hexanes. The precipitated solid was filtered through a sintered glass frit and rinsed with hexanes (2 × 15 mL). It was dried under high vacuum affording the title compound (11.13 g, 100% yield) as a beige crystalline solid. <sup>1</sup>H NMR (CDCl<sub>3</sub>): δ 12.05 (s, 1 H), 8.76 (s, 1 H), 8.26 (s, 1 H), 7.47 (m, 1 H), 7.10 (m, 2 H), 4.51 (m, 2 H), 1.47 (m, 3 H). MS (ESI, pos.ion) *m/z*: 320.0 (M+1). HPLC (Method B): retention time 5.95 min.

A similar procedure was used to prepare compounds **8a–e** and **8n**.

**Ethyl 6-Oxo-1-*o*-tolyl-6,7-dihydro-1H-pyrazolo[3,4-*b*]pyridine-5-carboxylate (8a).** <sup>1</sup>H NMR (CDCl<sub>3</sub>): δ 11.95 (s, 1 H), 8.75 (s, 1 H), 8.18 (s, 1 H), 7.28–7.44 (m, 4 H), 4.50 (q, *J* = 7.4 Hz, 2 H), 2.16 (s, 1 H), 1.47 (t, *J* = 7.3 Hz, 3 H). MS (ESI, pos.ion) *m/z*: 298.1 (M+1). HPLC (Method A): retention time 2.21 min.

**Ethyl 1-(2-Chlorophenyl)-6-oxo-6,7-dihydro-1H-pyrazolo[3,4-*b*]pyridine-5-carboxylate (8b).** <sup>1</sup>H NMR (CDCl<sub>3</sub>): δ 11.98

(s, 1 H), 8.75 (s, 1 H), 8.21 (s, 1 H), 7.59–7.52 (m, 2 H), 7.46–7.40 (m, 2 H), 4.51 (m, 2 H), 1.47 (m, 3 H). MS (ESI, pos.ion) *m/z*: 318.0 (M+1). HPLC (Method B): retention time 6.10 min.

**Ethyl 6-Oxo-1-(3-(trifluoromethyl)pyridin-2-yl)-6,7-dihydro-1H-pyrazolo[3,4-*b*]pyridine-5-carboxylate (8c).** <sup>1</sup>H NMR (CDCl<sub>3</sub>): δ 12.01 (s, 1 H), 8.86 (d, *J* = 3.5 Hz, 1 H), 8.76 (s, 1 H), 8.22–8.28 (m, 1 H), 8.21 (s, 1 H), 7.62 (dd, *J* = 7.8, 4.8 Hz, 1 H), 4.49 (q, *J* = 7.0 Hz, 2 H), 1.47 (t, *J* = 7.3 Hz, 3 H). MS (ESI, pos.ion) *m/z*: 353.0 (M+1). HPLC (Method A): retention time 1.93 min.

**Ethyl 1-(2,4-Difluorophenyl)-6-oxo-6,7-dihydro-1H-pyrazolo[3,4-*b*]pyridine-5-carboxylate (8d).** <sup>1</sup>H NMR (CDCl<sub>3</sub>): δ 12.03 (s, 1 H), 8.75 (s, 1 H), 8.21 (s, 1 H), 7.62 (td, *J* = 8.5, 6.0 Hz, 1 H), 7.00–7.09 (m, 2 H), 4.50 (q, *J* = 7.0 Hz, 2 H), 1.48 (t, *J* = 7.4 Hz, 3 H). MS (ESI, pos.ion) *m/z*: 320.0 (M+1). HPLC (Method B): retention time 6.13 min.

**Ethyl 1-(2,5-Difluorophenyl)-6-oxo-6,7-dihydro-1H-pyrazolo[3,4-*b*]pyridine-5-carboxylate (8e).** <sup>1</sup>H NMR (DMSO-*d*<sub>6</sub>): δ 12.10 (s, 1 H), 8.75 (s, 1 H), 8.40 (s, 1 H), 7.68 (m, 1 H), 7.58 (m, 1 H), 7.47 (m, 1 H), 4.34 (m, 2 H), 1.34 (m, 3 H). MS (ESI, pos.ion) *m/z*: 320.1 (M+1). HPLC (Method C): retention time 3.18 min.

**5-Amino-1-(2-fluorophenyl)-1H-pyrazole-4-carbaldehyde (8n).** <sup>1</sup>H NMR (CDCl<sub>3</sub>): δ 12.01 (s, 1 H), 8.75 (s, 1 H), 8.22 (s, 1 H), 7.65 (t, *J* = 7.0 Hz, 1 H), 7.43 (m, 1 H), 7.30 (m, 2 H), 4.50 (q, *J* = 7.0 Hz, 2 H), 1.34 (t, *J* = 7.0 Hz, 3 H). MS (ESI, pos.ion) *m/z*: 301.0 (M+1).

**5-Bromo-1-(2,6-difluorophenyl)-1H-pyrazolo[3,4-*b*]pyridin-6(7H)-one (9f).** A mixture of ethyl 1-(2,6-difluorophenyl)-6-oxo-6,7-dihydro-1H-pyrazolo[3,4-*b*]pyridine-5-carboxylate (**8f**) (9.40 g, 29 mmol) in acetonitrile (80 mL) and water (80 mL) at RT was treated with lithium hydroxide monohydrate (3.10 g, 74 mmol). The resulting suspension was heated at 90 °C in an oil bath for 1 h. It was cooled to 35 °C and treated with *N*-bromosuccinimide (5.20 g, 29 mmol) in one portion. The reaction mixture was allowed to stir for 1 h at RT then treated with additional *N*-bromosuccinimide (5.20 g, 29 mmol) in one portion. After stirring for 1 h at RT, the reaction mixture was treated with a saturated solution of NaHCO<sub>3</sub> and extracted with 2 × 150 mL EtOAc. The combined organic solution was washed with 15 mL of water followed by 15 mL of brine, dried over MgSO<sub>4</sub>, filtered, and concentrated to afford the title compound (8.31 g, 88% yield) as an orange amorphous solid. <sup>1</sup>H NMR (DMSO-*d*<sub>6</sub>): δ 12.63 (s, 1 H), 8.50 (s, 1 H), 8.22 (s, 1 H), 7.69 (m, 1 H), 7.42 (m, 2 H). MS (ESI, pos.ion) *m/z*: 325.9/327.9 (M+1). HPLC (Method B): retention time 5.05 min.

A similar procedure was used to prepare compounds **9a–e** and **9n**.

**5-Bromo-1-*o*-tolyl-1H-pyrazolo[3,4-*b*]pyridin-6(7H)-one (9a).** <sup>1</sup>H NMR (CDCl<sub>3</sub>): δ 9.43 (s, 1 H), 8.15 (s, 1 H), 7.85 (s, 1 H), 7.35–7.52 (m, 3 H), 7.29–7.34 (m, 1 H), 2.14 (s, 3 H). MS (ESI, pos.ion) *m/z*: 304.0/305.9 (M+1). HPLC (Method A): retention time 1.58 min.

**5-Bromo-1-(2-chlorophenyl)-1H-pyrazolo[3,4-*b*]pyridin-6(7H)-one (9b).** <sup>1</sup>H NMR (DMSO-*d*<sub>6</sub>): δ 12.50 (s, 1 H), 8.48 (s, 1 H), 8.13 (s, 1 H), 7.70 (dd, *J* = 1.4, 7.8 Hz, 1 H), 7.66–7.54 (m, 3 H). MS (ESI, pos.ion) *m/z*: 324.0/326.0 (M+1). HPLC (Method C): retention time 2.88 min.

**5-Bromo-1-(3-(trifluoromethyl)pyridin-2-yl)-1H-pyrazolo[3,4-*b*]pyridin-6(7H)-one (9c).** <sup>1</sup>H NMR (CDCl<sub>3</sub>): δ 11.47 (s, 1 H), 8.73 (d, *J* = 4.0 Hz, 1 H), 8.32 (d, *J* = 7.5 Hz, 1 H), 8.15 (s, 1 H), 7.88 (s, 1 H), 7.41–7.55 (m, 1 H). MS (ESI, pos.ion) *m/z*: 358.9/360.9 (M+1). HPLC (Method C): retention time 1.71 min.

**5-Bromo-1-(2,4-difluorophenyl)-1H-pyrazolo[3,4-*b*]pyridin-6(7H)-one (9d).** <sup>1</sup>H NMR (DMSO-*d*<sub>6</sub>): δ 12.66 (br., 1 H), 8.48 (s, 1 H), 8.15 (s, 1 H), 7.74 (td, *J* = 8.8, 6.2 Hz, 1 H), 7.55–7.63 (m, 1 H), 7.31 (t, *J* = 8.4 Hz, 1 H). MS (ESI, pos.ion) *m/z*: 325.9/327.9 (M+1). HPLC (Method B): retention time 5.43 min.

**5-Bromo-1-(2,5-difluorophenyl)-1H-pyrazolo[3,4-*b*]pyridin-6(7H)-one (9e).** MS (ESI, pos.ion) *m/z*: 326.0/328.0 (M+1). HPLC (Method C): retention time 2.63 min.



**5-Bromo-1-(2-difluorophenyl)-1H-pyrazolo[3,4-*b*]pyridin-6(7H)-one (9n).**  $^1\text{H}$  NMR (DMSO- $d_6$ ):  $\delta$  12.62 (br, 1 H), 8.48 (s, 1 H), 8.15 (s, 1 H), 7.66 (t,  $J$  = 8.8 Hz, 1 H), 7.49 (m, 2 H), 7.40 (t,  $J$  = 7.6 Hz, 1 H). MS (ESI, pos.ion)  $m/z$ : 307.9/309.9 (M+1). HPLC (Method A): retention time 1.56 min.

**5-Bromo-1-(2,6-difluorophenyl)-7-methyl-1H-pyrazolo[3,4-*b*]pyridin-6(7H)-one (10f).** At 0 °C, a solution of 5-bromo-1-(2,6-difluorophenyl)-1H-pyrazolo[3,4-*b*]pyridin-6(7H)-one (9f) (11.3 g, 34.7 mmol) in DME (78 mL) and DMF (7.7 mL) was treated with sodium hydride (1.24 g of 95% wt., 49 mmol) in small portions and the solution was allowed to stir at 0 °C for 10 min. Finely ground lithium bromide (8.83 g, 102 mmol) was then added and the solution stirred at RT for 20 min at which point iodo-methane (4.37 mL, 68.9 mmol) was added. The suspension was heated at 40 °C for 16 h then cooled to RT. The reaction mixture was quenched with ice cold water (25 mL) slowly and extracted with EtOAc (3  $\times$  100 mL). The combined organic solution was washed with 2  $\times$  20 mL of brine, dried over  $\text{MgSO}_4$ , filtered, and concentrated. The resulting crude solid was then suspended in 300 mL of 1:1 solution of EtOAc/hexanes with stirring over 30 min. The solution was allowed to precipitate in the freezer for 2 h. The resulting solid was collected by filtration washing with 2  $\times$  30 mL of methyl *t*-butyl ether to afford the title compound (5.27 g) in >95% purity as a beige solid. The mother liquor was and concentrated to ca. 15 mL in vacuo and treated with 50 mL of MTBE and again chilled in the freezer overnight. The resulting solid was collected by filtration followed by washing with 2  $\times$  10 mL of methyl *t*-butyl ether to afford a second crop (2.54 g) in >95% purity.  $^1\text{H}$  NMR ( $\text{CDCl}_3$ ):  $\delta$  8.09 (s, 1 H), 7.91 (s, 1 H), 7.56 (m, 1 H), 7.15 (m, 2 H), 3.39 (s, 3 H). MS (ESI, pos.ion)  $m/z$ : 340.0/342.0 (M+1). HPLC (Method B): retention time 5.37 min.

A similar procedure was used to prepare compounds 10a–e and 10n.

**5-Bromo-7-methyl-1-*o*-tolyl-1H-pyrazolo[3,4-*b*]pyridin-6(7H)-one (10a).**  $^1\text{H}$  NMR ( $\text{CDCl}_3$ ):  $\delta$  (s, 1 H), 7.83 (s, 1 H), 7.43–7.50 (m, 1 H), 7.34–7.40 (m, 3 H), 3.21 (s, 3 H), 2.05 (s, 3 H). MS (ESI, pos.ion)  $m/z$ : 317.9/320.0 (M+1). HPLC (Method A): retention time 1.83 min.

**5-Bromo-1-(2-chlorophenyl)-7-methyl-1H-pyrazolo[3,4-*b*]pyridin-6(7H)-one (10b).**  $^1\text{H}$  NMR ( $\text{CDCl}_3$ ):  $\delta$  8.09 (s, 1 H), 7.85 (s, 1 H), 7.62–7.46 (m, 4 H), 3.29 (s, 3 H). MS (ESI, pos.ion)  $m/z$ : 337.9/339.9 (M+1). HPLC (Method B): retention time 5.49 min.

**5-Bromo-7-methyl-1-(3-(trifluoromethyl)pyridin-2-yl)-1H-pyrazolo[3,4-*b*]pyridin-6(7H)-one (10c).**  $^1\text{H}$  NMR ( $\text{CDCl}_3$ ):  $\delta$  8.81 (d,  $J$  = 4.7 Hz, 1 H), 8.26–8.34 (m, 1 H), 8.11 (s, 1 H), 7.88 (s, 1 H), 7.71 (dd,  $J$  = 7.7, 5.0 Hz, 1 H), 3.24 (s, 3 H). MS (ESI, pos.ion)  $m/z$ : 372.8/374.9 (M+1). HPLC (Method A): retention time 1.71 min.

**5-Bromo-1-(2,4-difluorophenyl)-7-methyl-1H-pyrazolo[3,4-*b*]pyridin-6(7H)-one (10d).**  $^1\text{H}$  NMR ( $\text{CDCl}_3$ ):  $\delta$  8.08 (s, 1 H), 7.84 (s, 1 H), 7.58 (td,  $J$  = 8.5, 6.0 Hz, 1 H), 7.02–7.14 (m, 2 H), 3.36 (s, 3 H). MS (ESI, pos.ion)  $m/z$ : 339.9/341.9 (M+1). HPLC (Method B): retention time 5.31 min.

**5-Bromo-1-(2,5-difluorophenyl)-7-methyl-1H-pyrazolo[3,4-*b*]pyridin-6(7H)-one (10e).**  $^1\text{H}$  NMR (DMSO- $d_6$ ):  $\delta$  8.43 (s, 1 H), 8.08 (s, 1 H), 7.81 (m, 1 H), 7.60 (m, 2 H), 3.24 (s, 3 H). MS (ESI, pos.ion)  $m/z$ : 340.0/342.0 (M+1). HPLC (Method C): retention time 2.78 min.

**5-Bromo-1-(2-fluorophenyl)-7-methyl-1H-pyrazolo[3,4-*b*]pyridin-6(7H)-one (10n).**  $^1\text{H}$  NMR (DMSO- $d_6$ ):  $\delta$  8.43 (s, 1 H), 8.06 (s, 1 H), 7.78 (t,  $J$  = 7.8 Hz, 1 H), 7.67 (m, 1 H), 7.53 (t,  $J$  = 9.0 Hz, 1 H), 7.44 (t,  $J$  = 7.7 Hz, 1 H), 3.19 (s, 3 H). MS (ESI, pos.ion)  $m/z$ : 321.9/323.9 (M+1). HPLC (Method A): retention time 1.73 min.

***N*-Cyclopropyl-3-(1-(2,6-difluorophenyl)-7-methyl-6-oxo-6,7-dihydro-1H-pyrazolo[3,4-*b*]pyridin-5-yl)-4-methylbenzamide (3f).** A mixture of 5-bromo-1-(2,6-difluorophenyl)-7-methyl-1H-pyrazolo[3,4-*b*]pyridin-6(7H)-one (10f) (83.0 mg, 0.24 mmol), potassium phosphate (155 mg, 0.73 mmol), *N*-cyclopropyl-4-methyl-3-(4,4,5,5-tetramethyl-1,3,2-dioxaborolan-2-yl)benzamide (88 mg, 0.29 mmol),

X-Phos (7 mg) and tris(dibenzylideneacetone)dipalladium (0) (6.7 mg) in 2.0 mL of dioxane and 1.0 mL of water in a sealed glass tube was heated in a microwave at 135 °C for 30 min. The reaction mixture was partitioned between 10 mL of EtOAc and 1 mL of 1 N NaOH. The organic layer was washed with 1 mL of brine, dried over  $\text{MgSO}_4$ , filtered, and concentrated. Purification on a silica gel column (eluted with 40–90% EtOAc in hexanes) afforded the title compound (76.3 mg, 72% yield) as a white fluffy amorphous solid.  $^1\text{H}$  NMR ( $\text{CDCl}_3$ ):  $\delta$  7.97 (s, 1 H), 7.66 (m, 2 H), 7.56 (m, 2 H), 7.33 (d,  $J$  = 8.0 Hz, 1 H), 7.17 (t,  $J$  = 8.0 Hz, 2 H), 6.20 (br, 1 H), 3.49 (s, 3 H), 2.88 (m, 1 H), 2.29 (s, 3 H), 0.85 (m, 2 H), 0.59 (m, 2 H). MS (ESI, pos.ion)  $m/z$ : 435.1 (M+1). HPLC (Method A): retention time 1.84 min. HPLC (Method B): retention time 5.67 min.

A similar procedure was used to prepare compounds 3a–e and 3n.

***N*-Cyclopropyl-4-methyl-3-(7-methyl-6-oxo-1-*o*-tolyl-6,7-dihydro-1H-pyrazolo[3,4-*b*]pyridin-5-yl)benzamide (3a).**  $^1\text{H}$  NMR (methanol- $d_4$ ):  $\delta$  8.07 (s, 1 H), 7.89 (s, 1 H), 7.74 (d,  $J$  = 8.0 Hz, 1 H), 7.66 (s, 1 H), 7.53–7.61 (m, 2 H), 7.42–7.53 (m, 2 H), 7.38 (d,  $J$  = 8.0 Hz, 1 H), 3.24 (s, 3 H), 2.86 (m, 1 H), 2.28 (s, 3 H), 2.13 (s, 3 H), 0.78–0.85 (m, 2 H), 0.60–0.67 (m, 2 H). MS (ESI, pos.ion)  $m/z$ : 413.1 (M+1). HPLC (Method A): retention time 1.90 min. HPLC (Method B): retention time 5.31 min.

**3-(1-(2-Chlorophenyl)-7-methyl-6-oxo-6,7-dihydro-1H-pyrazolo[3,4-*b*]pyridin-5-yl)-*N*-cyclopropyl-4-methylbenzamide (3b).**  $^1\text{H}$  NMR ( $\text{CDCl}_3$ ):  $\delta$  7.91 (s, 1 H), 7.67 (m, 3 H), 7.60 (m, 1 H), 7.57–7.44 (m, 3 H), 7.31 (d,  $J$  = 8.0 Hz, 1 H), 6.25 (br, 1 H), 3.28 (s, 3 H), 2.89 (m, 1 H), 2.28 (s, 3 H), 0.85 (m, 2 H), 0.59 (m, 2 H). MS (ESI, pos.ion)  $m/z$ : 433.2 (M+1). HPLC (Method A): retention time 1.88 min. HPLC (Method B): retention time 5.55 min.

***N*-Cyclopropyl-4-methyl-3-(7-methyl-6-oxo-1-(3-(trifluoromethyl)pyridin-2-yl)-6,7-dihydro-1H-pyrazolo[3,4-*b*]pyridin-5-yl)benzamide (3c).**  $^1\text{H}$  NMR ( $\text{CDCl}_3$ ):  $\delta$  8.83 (dd,  $J$  = 4.8, 1.5 Hz, 1 H), 8.32 (dd,  $J$  = 8.0, 1.6 Hz, 1 H), 7.92–7.96 (m, 1 H), 7.64–7.74 (m, 3 H), 7.55 (d,  $J$  = 1.8 Hz, 1 H), 7.32 (d,  $J$  = 8.0 Hz, 1 H), 6.21 (br, 1 H), 3.23 (s, 3 H), 2.89 (td,  $J$  = 7.0, 3.3 Hz, 1 H), 2.29 (s, 3 H), 0.81–0.89 (m, 2 H), 0.55–0.63 (m, 2 H). MS (ESI, pos.ion)  $m/z$ : 468.0 (M+1). HPLC (Method A): retention time 1.80 min.

***N*-Cyclopropyl-3-(1-(2,4-difluorophenyl)-7-methyl-6-oxo-6,7-dihydro-1H-pyrazolo[3,4-*b*]pyridin-5-yl)-4-methylbenzamide (3d).**  $^1\text{H}$  NMR (methanol- $d_4$ ):  $\delta$  8.09 (s, 1 H), 7.88 (s, 1 H), 7.84 (td,  $J$  = 8.7, 5.8 Hz, 1 H), 7.74 (d,  $J$  = 8.0 Hz, 1 H), 7.66 (s, 1 H), 7.34–7.41 (m, 2 H), 7.28 (t,  $J$  = 8.3 Hz, 1 H), 3.38 (s, 3 H), 2.86 (dt,  $J$  = 7.0, 3.5 Hz, 1 H), 2.27 (s, 3 H), 0.77–0.85 (m, 2 H), 0.61–0.67 (m, 2 H). MS (ESI, pos.ion)  $m/z$ : 435.1 (M+1). HPLC (Method A): retention time 1.86 min. HPLC (Method C): retention time 2.84 min.

***N*-Cyclopropyl-3-(1-(2,5-difluorophenyl)-7-methyl-6-oxo-6,7-dihydro-1H-pyrazolo[3,4-*b*]pyridin-5-yl)-4-methylbenzamide (3e).**  $^1\text{H}$  NMR (DMSO- $d_6$ ):  $\delta$  8.35 (d,  $J$  = 3.9 Hz, 1 H), 8.13 (s, 1 H), 7.86 (s, 1 H), 7.73 (d,  $J$  = 7.9 Hz, 1 H), 7.65–7.59 (m, 4 H), 7.32 (d,  $J$  = 7.8 Hz, 1 H), 3.32 (s, 3 H), 2.84 (m, 1 H), 2.19 (s, 3 H), 0.68 (m, 2 H), 0.59 (m, 2 H). MS (ESI, pos.ion)  $m/z$ : 435.0 (M+1). HPLC (Method A): retention time 1.86 min.

***N*-Cyclopropyl-3-(1-(2-fluorophenyl)-7-methyl-6-oxo-6,7-dihydro-1H-pyrazolo[3,4-*b*]pyridin-5-yl)-4-methylbenzamide (3n).**  $^1\text{H}$  NMR (DMSO- $d_6$ ):  $\delta$  8.34 (d,  $J$  = 4.1 Hz, 1 H), 8.10 (s, 1 H), 7.96 (s, 1 H), 7.84 (t,  $J$  = 7.9 Hz, 1 H), 7.74–7.65 (m, 3 H), 7.54 (t,  $J$  = 9.5 Hz, 1 H), 7.46 (t,  $J$  = 7.7 Hz, 1 H), 7.32 (d,  $J$  = 8.0 Hz, 1 H), 3.20 (s, 3 H), 2.85 (m, 1 H), 2.19 (s, 3 H), 0.67 (m, 2 H), 0.56 (m, 2 H). MS (ESI, pos.ion)  $m/z$ : 417.0 (M+1). HPLC (Method A): retention time 1.80 min. HPLC (Method C): retention time 1.81 min.

**3-(1-(2,6-Difluorophenyl)-7-methyl-6-oxo-6,7-dihydro-1H-pyrazolo[3,4-*b*]pyridin-5-yl)-4-methylbenzoic acid (16).** A mixture of 5-bromo-1-(2,6-difluorophenyl)-7-methyl-1H-pyrazolo[3,4-*b*]pyridin-6(7H)-one (10f) (717 mg, 2.10 mmol), 3-boron-4-methylbenzoic acid (14) (455 mg, 2.53 mmol), and tetrakis(triphenylphosphine)palladium (0) (73 mg, 0.06 mmol) in dioxane (10 mL) and sodium carbonate (5.2 mL of 1 N solution) in a sealed glass

tube was heated in a microwave at 125 °C for 30 min. The reaction mixture was treated with 20 mL EtOAc and extracted 3 × 10 mL of 1 N NaOH. The organic solution was discarded. The combined aqueous solution was acidified with 5 N HCl to pH 4, and extracted with 3 × 75 mL of EtOAc. The combined EtOAc extracts were washed with 10 mL of brine, dried over MgSO<sub>4</sub>, filtered, and concentrated to afford the title compound (747 mg, 90% yield) as a white amorphous solid. <sup>1</sup>H NMR (DMSO-*d*<sub>6</sub>): δ 12.78 (br, 1 H), 8.18 (s, 1 H), 7.90 (s, 1 H), 7.88–7.60 (m, 2 H), 7.75 (s, 1 H), 7.49 (t, *J* = 8.5 Hz, 2 H), 7.39 (d, *J* = 8.0 Hz, 1 H), 3.26 (s, 3 H), 2.23 (s, 3 H). MS (ESI, pos.ion) *m/z*: 396.0 (M+1). HPLC (Method A): retention time 1.82 min. HPLC (Method B): retention time 5.65 min.

Alternative procedure for the synthesis of *N*-cyclopropyl-3-(1-(2,6-difluorophenyl)-7-methyl-6-oxo-6,7-dihydro-1*H*-pyrazolo[3,4-*b*]pyridin-5-yl)-4-methylbenzamide (**3f**). A solution of 3-(1-(2,6-difluorophenyl)-7-methyl-6-oxo-6,7-dihydro-1*H*-pyrazolo[3,4-*b*]pyridin-5-yl)-4-methylbenzoic acid (**16**) (1.69 g, 4.14 mmol) in THF (10.0 mL) at RT was treated with CDI (798 mg, 4.92 mmol) then heated at 50 °C for 1.5 h. It was cooled to RT and treated with cyclopropylamine (0.64 mL, 9.23 mmol). The reaction mixture was stirred at RT for 2 h then 50 °C for 2 h. It was then allowed to stir at RT overnight (16 h) resulting in a white suspension. The reaction mixture was partitioned between EtOAc (80 mL) and 1 N NaOH (15 mL). The organic layer was washed with brine, dried over MgSO<sub>4</sub>, filtered, and concentrated. Purification on a silica gel column (eluted with 40–90% EtOAc in hexanes) afforded *N*-cyclopropyl-3-(1-(2,6-difluorophenyl)-7-methyl-6-oxo-6,7-dihydro-1*H*-pyrazolo[3,4-*b*]pyridin-5-yl)-4-methylbenzamide (1.23 g, 69% yield) as a white fibrous solid. MS (ESI, pos.ion) *m/z*: 435.1 (M+1). HPLC (Method A): retention time 1.84 min. HPLC (Method B): retention time 5.67 min.

**5-Bromo-1-(2,4-difluorophenyl)-7-ethyl-1*H*-pyrazolo[3,4-*b*]pyridin-6(7*H*)-one (10g) and 5-bromo-1-(2,4-difluorophenyl)-6-ethoxy-1*H*-pyrazolo[3,4-*b*]pyridine (23).** A solution of 5-bromo-1-(2,4-difluorophenyl)-1*H*-pyrazolo[3,4-*b*]pyridin-6(7*H*)-one (**9c**) (500 mg, 1.53 mmol) in DME (10 mL) and DMF (1 mL) at 0 °C was treated with sodium hydride (368 mg of 60% wt. in mineral oil, 9.20 mmol) under argon. After stirring 20 min, lithium bromide (533 mg, 6.13 mmol) was added and the resulting suspension was allowed to stir for 30 min at RT before iodoethane (1.24 mL, 15.3 mmol) was added. The reaction mixture was heated at 40 °C in an oil bath for 24 h. The reaction mixture was quenched with ice-cold water (5 mL) and extracted with EtOAc (2 × 40 mL). The combined organic extracts were washed with brine (10 mL) and dried over MgSO<sub>4</sub>, filtered, and concentrated. The resulting crude residue was loaded on an ISCO 40 g column and eluted with 0–50% EtOAc in hexanes to give the 5-bromo-1-(2,4-difluorophenyl)-6-ethoxy-1*H*-pyrazolo[3,4-*b*]pyridine (**23**) (423 mg, 78% yield) as a white fibrous solid and the 5-bromo-1-(2,4-difluorophenyl)-7-ethyl-1*H*-pyrazolo[3,4-*b*]pyridin-6(7*H*)-one (**10g**) (92 mg, 17% yield) as a pale yellow viscous oil. Compound **23**: <sup>1</sup>H NMR (CDCl<sub>3</sub>): δ 8.19 (s, 1 H), 8.04 (s, 1 H), 7.62 (td, *J* = 8.6, 6.1 Hz, 1 H), 7.00–7.09 (m, 2 H), 4.43 (q, *J* = 7.0 Hz, 2 H), 1.43 (t, *J* = 7.1 Hz, 3 H). MS (ESI, pos.ion) *m/z*: 353.9/355.9 (M+1). HPLC (Method A): retention time 2.77 min. Compound **10g**: <sup>1</sup>H NMR (CDCl<sub>3</sub>): δ 8.07 (s, 1 H), 7.85 (s, 1 H), 7.58 (td, *J* = 8.4, 5.8 Hz, 1 H), 7.01–7.13 (m, 2 H), 4.02 (dq, *J* = 14.1, 7.0 Hz, 1 H), 3.82 (dq, *J* = 14.1, 7.2 Hz, 1 H), 1.03 (t, *J* = 7.0 Hz, 3 H). MS (ESI, pos.ion) *m/z*: 353.9/355.9 (M+1). HPLC (Method A): retention time 1.93 min.

***N*-Cyclopropyl-3-(1-(2,4-difluorophenyl)-7-ethyl-6-oxo-6,7-dihydro-1*H*-pyrazolo[3,4-*b*]pyridin-5-yl)-4-methylbenzamide (3g).** In a 5 mL glass microwave tube was weighed tetrakis(triphenylphosphine) palladium(0) (6.9 mg, 5.9 μmol), *N*-cyclopropyl-4-methyl-3-(4,4,5,5-tetramethyl-1,3,2-dioxaborolan-2-yl)benzamide (65 mg, 0.22 mmol) and 5-bromo-1-(2,4-difluorophenyl)-7-ethyl-1*H*-pyrazolo[3,4-*b*]pyridin-6(7*H*)-one (**10g**) (70.0 mg, 0.20 mmol). The solids were purged with argon and treated with 1,4-dioxane (1.5 mL), 1 M sodium carbonate (0.40 mL, 0.40 mmol), and heated

in a microwave at 130 °C for 30 min. The reaction mixture was treated with brine and extracted EtOAc (2 × 15 mL), dried over MgSO<sub>4</sub>, filtered, and concentrated. Purification on the ISCO (12 g column, 20–80% EtOAc in hexanes) afforded the title compound (54 mg, 61% yield) as a white amorphous solid. <sup>1</sup>H NMR (CDCl<sub>3</sub>): δ 7.91 (s, 1 H), 7.60–7.67 (m, 3 H), 7.57 (s, 1 H), 7.31 (d, *J* = 8.0 Hz, 1 H), 7.04–7.15 (m, 2 H), 6.19 (br, 1 H), 3.97–4.09 (m, 1 H), 3.76–3.89 (m, 1 H), 2.89 (dd, *J* = 7.0, 3.5 Hz, 1 H), 2.28 (s, 3 H), 1.04 (m, 3 H), 0.81–0.89 (m, 2 H), 0.55–0.63 (m, 2 H). MS (ESI, pos.ion) *m/z*: 449.1 (M+1). HPLC (Method A): retention time 1.98 min. HPLC (Method B): retention time 5.88 min.

**4-Chloro-*N*-cyclopropyl-3-(1-(2,6-difluorophenyl)-7-methyl-6-oxo-6,7-dihydro-1*H*-pyrazolo[3,4-*b*]pyridin-5-yl)benzamide (3i).** In a 25 mL microwave tube was weighed 4-chloro-*N*-cyclopropyl-3-(4,4,5,5-tetramethyl-1,3,2-dioxaborolan-2-yl)benzamide (**12**) (129 mg, 0.40 mmol), 5-bromo-1-(2,6-difluorophenyl)-7-methyl-1*H*-pyrazolo[3,4-*b*]pyridin-6(7*H*)-one (**10f**) (119 mg, 0.35 mmol) and tetrakis(triphenylphosphine)palladium (0) (16 mg, 14 μmol). The solids were purged with argon and treated with sodium carbonate (0.88 mL of 1 M solution, 0.88 mmol) and 2.0 mL dioxane and heated to 130 °C in a microwave for 25 min. The reaction mixture was treated with 5 mL of water and extracted with 2 × 15 mL EtOAc. The combined organic solution was dried over MgSO<sub>4</sub>, filtered, and concentrated. Purification on the ISCO (12 g column, 40–90% EtOAc in hexanes) afforded the title compound (70 mg, 44% yield) as an off-white amorphous solid. <sup>1</sup>H NMR (CDCl<sub>3</sub>): δ 7.99 (s, 1 H), 7.75 (s, 1 H), 7.73 (m, 1 H), 7.70 (s, 1 H), 7.54 (m, 2 H), 7.17 (m, 2 H), 6.22 (br., 1 H), 3.39 (s, 3 H), 2.88 (m, 1 H), 0.86 (m, 2 H), 0.60 (m, 2 H). MS (ESI, pos.ion) *m/z*: 455.0 (M+1). HPLC (Method A): retention time 1.90 min. HPLC (Method B): retention time 5.67 min.

***N*-Cyclopropyl-3-(1-(2,6-difluorophenyl)-7-methyl-6-oxo-6,7-dihydro-1*H*-pyrazolo[3,4-*b*]pyridin-5-yl)-5-fluoro-4-methylbenzamide (3j).** A mixture of 5-bromo-1-(2,6-difluorophenyl)-7-methyl-1*H*-pyrazolo[3,4-*b*]pyridin-6(7*H*)-one (**10f**) (110 mg, 0.32 mmol), *N*-cyclopropyl-3-fluoro-4-methyl-5-(4,4,5,5-tetramethyl-1,3,2-dioxaborolan-2-yl)benzamide (**13**) (122 mg, 0.38 mmol), tetrakis(triphenylphosphine) palladium (0) (15 mg, 12 μmol) in 2.0 mL of dioxane and 0.8 mL of 1 M sodium carbonate was heated in a microwave at 130 °C for 45 min. The reaction mixture was diluted with 5 mL of water and extracted with EtOAc (2 × 15 mL). The combined organic extracts were dried over MgSO<sub>4</sub>, filtered, and concentrated. Purification on the ISCO (12 g column, 40–80% EtOAc in hexanes) afforded the title compound (96 mg, 65% yield) as a light yellow amorphous solid. <sup>1</sup>H NMR (methanol-*d*<sub>4</sub>) δ 8.16 (s, 1 H), 7.94 (s, 1 H), 7.72–7.82 (m, 1 H), 7.51–7.59 (m, 2 H), 7.36 (t, *J* = 8.5 Hz, 2 H), 3.41 (s, 3 H), 2.86 (dt, *J* = 7.4, 3.6 Hz, 1 H), 2.17 (s, 3 H), 0.78–0.85 (m, 2 H), 0.60–0.68 (m, 2 H). MS (ESI, pos.ion) *m/z*: 453.0 (M+1). HPLC (Method A): retention time 1.97 min. HPLC (Method B): retention time 5.82 min.

**3-(1-(2,6-Difluorophenyl)-7-methyl-6-oxo-6,7-dihydro-1*H*-pyrazolo[3,4-*b*]pyridin-5-yl)-4-methylbenzamide (3k).** To a slurry of 3-(1-(2,6-difluorophenyl)-7-methyl-6-oxo-6,7-dihydro-1*H*-pyrazolo[3,4-*b*]pyridin-5-yl)-4-methylbenzoic acid (**16**) (2.72 g, 6.88 mmol) in THF (15 mL) at RT was added 1,1'-carbonyldiimidazole (2.10 g, 13.0 mmol). After stirring at RT for 2 h, the heterogeneous mixture turned into a homogeneous clear solution. To the reaction mixture at RT was added in ammonia (70 mL of 0.5 M solution in 1,4-dioxane, 35 mmol). After stirring at RT for 18 h, the reaction mixture was diluted with EtOAc (100 mL), washed sequentially with 1 N NaOH (15 mL) and brine (15 mL). The organic layer was dried and concentrated. Purification on an ISCO (40 g column, eluted with 50–100% EtOAc in CH<sub>2</sub>Cl<sub>2</sub>) afforded 3-(1-(2,6-difluorophenyl)-7-methyl-6-oxo-6,7-dihydro-1*H*-pyrazolo[3,4-*b*]pyridin-5-yl)-4-methylbenzamide (2.22 g, 82% yield) as an off-white crystalline solid. <sup>1</sup>H NMR (CDCl<sub>3</sub>): δ 7.98 (s, 1 H), 7.73 (dd, *J* = 7.8, 1.9 Hz, 1 H), 7.67 (s, 2 H), 7.58 (m, 1 H), 7.36 (d, *J* = 8.0 Hz, 1 H), 7.16 (m, 2 H), 6.10 (br, 1 H), 5.60 (br, 1 H), 3.39 (s, 3 H), 2.31 (s, 3 H). MS (ESI, pos.ion) *m/z*: 395.1 (M+1). HPLC (Method A): retention time 1.62 min. HPLC (Method C): retention time 1.80 min.



**3-(1-(2,6-Difluorophenyl)-7-methyl-6-oxo-6,7-dihydro-1H-pyrazolo[3,4-*b*]pyridin-5-yl)-*N*-(isoxazol-3-yl)-4-methylbenzamide (3m).** At RT, 3-(1-(2,6-difluorophenyl)-7-methyl-6-oxo-6,7-dihydro-1H-pyrazolo[3,4-*b*]pyridin-5-yl)-4-methylbenzoic acid (**16**) (74.0 mg, 0.18 mmol) was treated with thionyl chloride (3.0 mL, 41.1 mmol) and the resulting mixture heated at 95 °C in an oil bath for 2 h. The excess thionyl chloride was removed in vacuo. The remaining crude acid chloride was dissolved in 3 mL of CH<sub>2</sub>Cl<sub>2</sub> and then added slowly to another reaction vessel at RT which contained a mixture of 4-(dimethylamino) pyridine (23 mg, 0.18 mmol), 3-aminoisoxazole (24 mg, 0.28 mmol), Hunig's base (0.065 mL, 0.37 mmol) in CH<sub>2</sub>Cl<sub>2</sub> (1.0 mL). The reaction mixture was allowed to stir at RT for 16 h. It was quenched with 0.5 N HCl (4 mL) and extracted with EtOAc (2 × 30 mL). The combined organic solution was washed with a saturated solution of NaHCO<sub>3</sub> and dried over MgSO<sub>4</sub>. Purification on the ISCO (12 g column, 30–80% EtOAc in hexanes) afforded the title compound (26.2 mg, 30% yield) as a white amorphous solid. <sup>1</sup>H NMR (CDCl<sub>3</sub>): δ 8.78 (s, 1 H), 8.30 (d, *J* = 1.6 Hz, 1 H), 7.99 (s, 1 H), 7.82 (dd, *J* = 7.8, 2.0 Hz, 1 H), 7.78 (d, *J* = 2.0 Hz, 1 H), 7.69 (s, 1 H), 7.53–7.63 (m, 1 H), 7.41 (d, *J* = 8.0 Hz, 1 H), 7.14–7.22 (m, 3 H), 3.40 (s, 3 H), 2.34 (s, 3 H). MS (ESI, pos.ion) *m/z*: 462.0 (M+1). HPLC (Method A): retention time 1.97 min. HPLC (Method B): retention time 5.80 min.

**3-(1-(2,6-Difluorophenyl)-7-methyl-6-oxo-6,7-dihydro-1H-pyrazolo[3,4-*b*]pyridin-5-yl)-4-methyl-*N*-(1-methylcyclopropyl)-benzamide (3l).** (43 mg, 76% yield) was prepared in a similar procedure to that described for **3m**. <sup>1</sup>H NMR (DMSO-*d*<sub>6</sub>): δ 8.55 (s, 1 H), 8.19 (s, 1 H), 7.87 (s, 1 H), 7.80 (m, 1 H), 7.72 (m, 1 H), 7.66 (s, 1 H), 7.49 (m, 2 H), 7.31 (d, *J* = 8.0 Hz, 1 H), 3.25 (s, 3 H), 2.18 (s, 3 H), 1.36 (s, 3 H), 0.71 (m, 2 H), 0.59 (m, 2 H). MS (ESI, pos.ion) *m/z*: 449.1 (M+1). HPLC (Method A): retention time 1.96 min. HPLC (Method C): retention time 2.00 min.

**1-(2,6-Difluorophenyl)-7-methyl-5-(6-methyl-3-(methylamino)-benzo[*d*]isoxazol-7-yl)-1H-pyrazolo[3,4-*b*]pyridin-6(7H)-one (17).** A mixture of 7-iodo-*N*,6-dimethylbenzo[*d*]isoxazol-3-amine (240 mg, 0.833 mmol), 4,4,5,5-tetramethyl-1,3,2-dioxaborolane (2.50 mL of 1.0 M THF solution, 2.50 mmol), triethylamine (0.464 mL, 3.33 mmol), 2-(dicyclohexylphosphino)-2'-methylbiphenyl (60 mg, 0.167 mmol), and palladium acetate (9.3 mg, 0.041 mmol) in 3.0 mL of dioxane in a sealed glass tube was heated in a microwave at 100 °C for 20 min. LC-MS of the crude reaction mixture indicated the formation of *N*,6-dimethylbenzo[*d*]isoxazol-3-amine [MS (ESI, pos.ion) *m/z*: 163.0 (M+1). HPLC (Method C): retention time 1.61 min] and *N*,6-dimethyl-7-(4,4,5,5-tetramethyl-1,3,2-dioxaborolan-2-yl)benzo[*d*]isoxazol-3-amine (**15**) [MS (ESI, pos.ion) *m/z*: 289.0 (M+1). HPLC (Method C): retention time 2.26 min.] in a ratio of 2:3. The crude reaction mixture was transferred via pipet to a 25 mL round-bottom flask which contained a solution of 5-bromo-1-(2,6-difluorophenyl)-7-methyl-1H-pyrazolo[3,4-*b*]pyridin-6(7H)-one (**10f**) (100 mg, 0.29 mmol) in 2.0 mL of dioxane. The mixture was cooled with an ice bath and sodium carbonate (10.00 mL of 1 M solution, 10.0 mmol) was added dropwise, which resulted in vigorous evolution of gas. After all the gas bubbles were gone, it was treated with tetrakis(triphenylphosphine)palladium (0) (17 mg, 0.015 mmol). The reaction mixture was heated in an oil bath at 110 °C for 5 h. After cooling to RT, it was diluted with 60 mL of EtOAc. The organic phase was separated and washed with saturated aqueous solution of sodium bicarbonate, followed by brine. The resulting organic solution was dried over magnesium sulfate and concentrated under reduced pressure. Purification by flash chromatography on silica gel (eluted with 50–100% EtOAc in CH<sub>2</sub>Cl<sub>2</sub>) gave 1-(2,6-difluorophenyl)-7-methyl-5-(6-methyl-3-(methylamino)benzo[*d*]isoxazol-7-yl)-1H-pyrazolo[3,4-*b*]pyridin-6(7H)-one (78 mg, 63% yield) as a white crystalline solid. <sup>1</sup>H NMR (CDCl<sub>3</sub>): δ 7.97 (s, 1 H), 7.81 (s, 1 H), 7.57 (m, 1 H), 7.27 (m, 1 H), 7.20 (m, 2 H), 7.07 (d, *J* = 8.0 Hz, 1 H), 4.50 (br, 1 H), 3.41 (s, 3 H), 3.04 (d, *J* = 5.1 Hz, 3 H), 2.35 (s, 3 H). SXU 84133–6 MS (ESI, pos.ion) *m/z*: 422.0 (M+1). HPLC (Method A): retention time 1.85 min.

**5-Amino-1-(2,6-difluorophenyl)-3-methyl-1H-pyrazole-4-carbonitrile (19).** (1-Ethoxyethylidene)malononitrile (**18**) (1.58 g, 11.6 mmol) was added in small portions to a solution of 1-(2,6-difluorophenyl)hydrazine hydrochloride (2.00 g, 11.1 mmol) and triethylamine (1.62 mL, 11.6 mmol) in 7 mL of EtOH at RT. The mixture was heated at reflux for 1 h. The reaction mixture was then concentrated and the residue was dissolved in EtOAc and washed with water followed by saturated NaHCO<sub>3</sub> (aq.). The combined organic layer was dried over anhydrous sodium sulfate, filtered, and concentrated to give the title compound (2.51 g, 97% yield) as a brown solid. <sup>1</sup>H NMR (CDCl<sub>3</sub>): δ 7.50 (m, 1 H), 7.13 (m, 2 H), 4.41 (br., 2 H), 2.34 (s, 3 H). MS (ESI, pos.ion) *m/z*: 235.1 (M+1).

**5-Amino-1-(2,6-difluorophenyl)-3-methyl-1H-pyrazole-4-carbaldehyde (20).** Raney 2800 nickel (slurry in water, 3.00 mL, 25.6 mmol) was added to a mixture of 5-amino-1-(2,6-difluorophenyl)-3-methyl-1H-pyrazole-4-carbonitrile (**19**) (2.15 g, 9.18 mmol) in 50 mL of 70% acetic acid and 15 mL of EtOH. The mixture was stirred under a positive pressure of hydrogen (40 psi) for 48 h. The reaction mixture was filtered through a pad of Celite and washed with wet EtOAc. The filtrate was transferred to a separatory funnel, layers were separated and the aqueous layer was extracted with EtOAc (3×). The combined organic layers were washed with 1 M NaOH (aq.) and brine and then dried over anhydrous sodium sulfate, filtered, and concentrated. The crude material was purified by silica gel chromatography (25–50% EtOAc in hexanes) to afford the title compound (1.70 g, 78% yield) as a light yellow solid. <sup>1</sup>H NMR (CDCl<sub>3</sub>): δ 9.72 (s, 1 H), 7.47 (m, 1 H), 7.11 (m, 2 H), 5.70 (br, 2 H), 2.42 (s, 3 H). MS (ESI, pos.ion) *m/z*: 238.1 (M+1).

**Ethyl 1-(2,6-difluorophenyl)-3-methyl-6-oxo-6,7-dihydro-1H-pyrazolo[3,4-*b*]pyridine-5-carboxylate Piperidine Salt (21).** A solution of 5-amino-1-(2,6-difluorophenyl)-3-methyl-1H-pyrazole-4-carbaldehyde (**20**) (1.04 g, 4.37 mmol) in 12 mL of EtOH was treated with diethyl malonate (2.66 mL, 8.74 mmol) and piperidine (0.86 mL, 8.74 mmol) and heated to reflux for 20 h. The reaction mixture was concentrated and 10 mL of 1/1 mixture of EtOAc/hexanes was added to the beige solid and it was filtered. The solid was washed with hexanes (25 mL) to afford the title compound (1.57 g, 86% yield) as a white solid. <sup>1</sup>H NMR (CD<sub>3</sub>OD): δ 8.49 (s, 1 H), 7.57 (m, 1 H), 7.20 (m, 2 H), 4.36 (q, *J* = 7.03 Hz, 2 H), 3.02 (m, 4 H), 2.51 (s, 3 H), 1.71 (m, 4 H), 1.64 (m, 2 H), 1.41 (t, *J* = 7.03 Hz, 3 H). MS (ESI, pos.ion) *m/z*: 334.1 (M+1). HPLC (Method A): retention time 2.26 min.

**5-Bromo-1-(2,6-difluorophenyl)-3,7-dimethyl-1H-pyrazolo[3,4-*b*]pyridin-6(7H)-one (22).** A suspension of ethyl 1-(2,6-difluorophenyl)-3-methyl-6-oxo-6,7-dihydro-1H-pyrazolo[3,4-*b*]pyridine-5-carboxylate piperidine salt (**21**) (1.04 g, 3.14 mmol) in 16 mL of 1/1 mixture of MeCN/H<sub>2</sub>O was treated with LiOH monohydrate (0.336 g, 8.00 mmol) and heated to 90 °C for 2 h. The reaction mixture was allowed to cool to RT and *N*-bromosuccinimide (1.12 g, 6.28 mmol) was added and the mixture was stirred for 2 h at RT. Saturated NaHCO<sub>3</sub> (aq.) was added and the mixture was extracted with EtOAc (3×). The combined organic layers were dried over anhydrous Na<sub>2</sub>SO<sub>4</sub>, filtered and concentrated to give 5-bromo-1-(2,6-difluorophenyl)-3-methyl-1H-pyrazolo[3,4-*b*]pyridin-6(7H)-one (852 mg, 80% yield) as a brown syrup. MS (ESI, pos.ion) *m/z*: 340.0/342.0 (M+1).

A solution of 5-bromo-1-(2,6-difluorophenyl)-3-methyl-1H-pyrazolo[3,4-*b*]pyridin-6(7H)-one (475 mg, 1.40 mmol) in 2.5 mL of 10/1 mixture of DME/DMF at 0 °C was treated with NaH (60% wt. in mineral oil, 78 mg, 1.96 mmol). The mixture was allowed to stir for 10 min at 0 °C and then LiBr (358 mg, 4.12 mmol) was added and the mixture was allowed to stir for 20 min at RT. MeI (0.174 mL, 2.79 mmol) was added, and the reaction was heated at 40 °C for 16 h. The mixture was allowed to cool to RT, water was added, and the mixture was extracted with EtOAc (3×). The combined organic layers were dried over anhydrous sodium sulfate, filtered, and concentrated. The crude product was purified by silica gel chromatography (10–60%

EtOAc in hexanes) to afford the title compound (120 mg, 24% yield) as a yellow solid.  $^1\text{H}$  NMR ( $\text{CD}_3\text{OD}$ ):  $\delta$  8.03 (s, 1 H), 7.54 (m, 1 H), 7.14 (m, 2 H), 3.37 (s, 3 H), 2.44 (s, 3 H). MS (ESI, pos. ion)  $m/z$ : 354.0/356.0 ( $\text{M}+1$ ).

***N*-Cyclopropyl-3-(1-(2,6-difluorophenyl)-3,7-dimethyl-6-oxo-6,7-dihydro-1*H*-pyrazolo[3,4-*b*]pyridin-5-yl)-4-methylbenzamide (3h).** In a microwave tube was placed 5-bromo-1-(2,6-difluorophenyl)-3,7-dimethyl-1*H*-pyrazolo[3,4-*b*]pyridin-6(7*H*)-one (**22**) (68 mg, 0.19 mmol), *N*-cyclopropyl-4-methyl-3-(4,4,5,5-tetramethyl-1,3,2-dioxaborolan-2-yl)benzamide (**11**) (75 mg, 0.25 mmol), tetrakis(triphenylphosphine)palladium (**0**) (11 mg, 0.0096 mmol) and  $\text{Na}_2\text{CO}_3$  (aq. 2 M solution, 0.48 mL, 0.96 mmol) in 2 mL of dioxane. The mixture was heated in a microwave at 120 °C for 25 min. Water was added, and the mixture was extracted with EtOAc (3 $\times$ ). The combined organic layers were dried over anhydrous sodium sulfate, filtered, and concentrated. The crude material was purified by silica gel chromatography (30–80% EtOAc in hexanes) to give the title compound (25 mg, 29% yield) as white needles.  $^1\text{H}$  NMR ( $\text{CD}_3\text{OD}$ ):  $\delta$  7.66 (m, 1 H), 7.55 (m, 3 H), 7.30 (m, 1 H), 7.15 (m, 2 H), 6.21 (br, 1 H), 3.36 (s, 3 H), 2.90 (m, 1 H), 2.46 (s, 3 H), 2.29 (s, 3 H), 0.86 (m, 2 H), 0.60 (m, 2 H). MS (ESI, pos.ion)  $m/z$ : 449.2 ( $\text{M}+1$ ). HPLC (Method A): retention time 1.90 min. HPLC (Method C): retention time 1.96 min.

**Biological Methods. p38 $\alpha$  MAP Kinase in Vitro Assay.** The p38 $\alpha$  kinase reaction was carried out in a polypropylene 96-well black round-bottomed assay plate in a total volume of 30  $\mu\text{L}$  kinase reaction buffer (50 mM Tris-pH 7.5, 5 mM  $\text{MgCl}_2$ , 0.1 mg/mL BSA, 100  $\mu\text{M}$   $\text{Na}_3\text{VO}_4$ , and 0.5 mM DTT). Recombinant activated human p38 enzyme (1 nM) was mixed with 50  $\mu\text{M}$  ATP and 100 nM GST-ATF2-Avitag, in the presence or absence of inhibitor. The reaction was allowed to incubate for 1 h at RT. The kinase reaction was terminated and phospho-ATF2 was revealed by addition of 30  $\mu\text{L}$  of HTRF detection buffer (100 mM HEPES, pH 7.5, 100 mM NaCl, 0.1% BSA, 0.05% Tween-20, and 10 mM EDTA) supplemented with 0.1 nM Eu-anti-pTP and 4 nM SA-APC. After 1 h incubation at RT, the assay plate was read in a Discovery Plate Reader (Perkin-Elmer). The wells were excited with coherent 320 nm light and the ratio of delayed (50 ms post excitation) emissions at 620 nm (native europium fluorescence) and 665 nm (europium fluorescence transferred to allophycocyanin, an index of substrate phosphorylation) was determined (reference: Park, Y. W.; Cummings, R. T.; Wu, L.; Cameron, P. M.; Woods, A.; Zaller, D. M.; Marcy, A. I.; Hermes, J. D. Homogeneous Proximity Tyrosine Kinase Assays: Scintillation Proximity Assay versus Homogeneous Time-Resolved Fluorescence. *Anal. Biochem.* **1999**, 269, 94–104). The proportion of substrate phosphorylated in the kinase reaction in the presence of compound compared with that phosphorylated in the presence of DMSO vehicle alone (HI control) was calculated using the formula: % control (POC) = (compd – average LO)/(average HI – average LO)  $\times$  100. Data (consisting of POC and inhibitor concentration in  $\mu\text{M}$ ) was fitted to a four-parameter equation ( $y = A + ((B - A)/(1 + ((x/C)^D)))$ ), where  $A$  is the minimum  $y$  (POC) value,  $B$  is the maximum  $y$  (POC),  $C$  is the  $x$  (compd concentration) at the point of inflection, and  $D$  is the slope factor) using a Levenberg–Marquardt nonlinear regression algorithm. The inhibition constant ( $K_i$ ) of the inhibitor was estimated from the  $\text{IC}_{50}$  (compd concentration at the point of inflection;  $C$ ) using the Cheng–Prussif equation:  $K_i = \text{IC}_{50}/(1 + S/K_m)$ , where  $S$  is the ATP substrate concentration, and  $K_m$  is the Michaelis constant for ATP as determined experimentally.

**LPS-Induced TNF- $\alpha$  Production in THP-1 Cells.** THP1 cells were resuspended in fresh THP1 media (RPMI 1640, 10% heat-inactivated FBS, 1  $\times$  PGS, 1  $\times$  NEAA, plus 30  $\mu\text{M}$   $\beta\text{ME}$ ) at a concentration of  $1.5 \times 10^6$  cells per mL. One hundred microliters of cells per well were plated in a flat-bottom polystyrene 96-well tissue culture plate. Two micrograms per milliliter of bacterial LPS (Sigma) was prepared in THP1 media and transferred to the first 11 columns of a 96-well polypropylene plate. Column

12 contained only THP1 media for the LO control. Compounds were dissolved in 100% DMSO and serially diluted 3-fold in a polypropylene 96-well microtiter plate (drug plate). Columns 6 and 12 were reserved as controls (HI control and LO control, respectively) and contained only DMSO. One microliter of inhibitor compound from the drug plate followed by 10  $\mu\text{L}$  of LPS was transferred to the cell plate. The treated cells were induced to synthesize and secrete TNF $\alpha$  in a 37 °C humidified incubator with 5%  $\text{CO}_2$  for 3 h. TNF $\alpha$  production was determined by transferring 50  $\mu\text{L}$  of conditioned media to a 96-well small spot TNF $\alpha$  plate (MSD – Meso Scale Discovery) containing 100  $\mu\text{L}$  of 2 $\times$  Read Buffer P supplemented with an anti-TNF $\alpha$  polyclonal Ab labeled with ruthenium (MSD-Sulfo-TAG – NHS ester). After overnight incubation at RT with shaking, the reaction was read on the Sector Imager 6000 (MSD). A low voltage was applied to the ruthenylated TNF $\alpha$  immune complexes, which in the presence of TPA (the active component in the ECL reaction buffer, Read Buffer P), resulted in a cyclical redox reaction generating light at 620 nm. The amount of secreted TNF $\alpha$  in the presence of compound compared with that in the presence of DMSO vehicle alone (HI control) was calculated using the formula: % control (POC) = (compd – average LO)/(average HI – average LO)  $\times$  100.

**TNF-Challenged IL-8 Production in Human Whole Blood Cells.** Whole blood was drawn from healthy, nonmedicated volunteers into sodium heparin tubes. 100  $\mu\text{L}$  of blood were then plated into 96 well tissue culture plates (BD). Ten point compound titrations were added to the blood and incubated for 1 h at 37 °C with 5%  $\text{CO}_2$ . TNF- $\alpha$  (Amgen) with a final concentration of 1 nM was then added to the blood and incubated overnight (16–18 h) at 37 °C with 5%  $\text{CO}_2$ . Plasma was harvested and cytokines (IL8) were measured by MSD (Meso Scale Discovery) ECL based antibody sandwich assay. All reagents were prepared in RPMI 1640, 10% v/v human serum AB (Gemini Bio-Products), 1 $\times$  Pen/Strep/Glu. Final concentration of human whole blood was 50%. Data were analyzed using XLfit/Activity Base software package (IDBS).

**LPS-Induced MK2 Phosphorylation in Human Whole Blood Cells.** Whole blood was drawn from healthy, nonmedicated volunteers into sodium heparin tubes. 60  $\mu\text{L}$  of the blood was aliquoted into 96-well deep well plate. Inhibitor was diluted at series of 3 $\times$  dilutions with RPMI medium plus 10% human serum. Ten point compound dilutions as well as no-compound control were added to the blood to make 50% blood as a final condition. Compounds were allowed to incubate with blood at RT for 30 min and LPS were added at a final concentration of 1  $\mu\text{g}/\text{mL}$  to each well; no LPS treated wells were kept as negative control for each set of series of dilutions. LPS activation was carried out at RT for 45 min and the reaction stopped by addition of 800  $\mu\text{L}$  of 37 °C PhosFlow Lyse/Fix buffer (BD, San Jose, CA) with vigorous shaking. Cells were kept in Lyse/Fix buffer at 37 °C for 30 min for complete fixation and permeabilized in 800  $\mu\text{L}$  ice cold 80% methanol on ice for no less than 2 h. Cells were then rinsed with PBS and stained with Alexa 647 conjugated antihuman pMK2 antibody (Cell Signaling, Danvers, MA) at 1:500 dilution. Levels of MK2 phosphorylation were determined by flow cytometry (FACS Calibur, BD, San Jose, CA) and presented as mean fluorescence intensity (MFI) of labeled cells. Results were expressed as POC of MFI and standard error of the MFI for duplicate measurements. Data were analyzed using GraphPad Prism 4.01 (GraphPad Software Inc. San Diego, CA).

**Acknowledgment.** The authors thank Randy Jensen and Chris Wilde for spectroscopic assistance.

**Supporting Information Available:** X-ray data of cocrystal of **3d** in p38 $\alpha$  protein is provided. This material is available free of charge via the Internet at <http://pubs.acs.org>.



## References

- (1) Han, J.; Lee, J. D.; Bibbs, L.; Ulevitch, R. J. A MAP kinase targeted by endotoxin and hyperosmolarity in mammalian cells. *Science* **1994**, *265*, 808–811.
- (2) (a) Raingeaud, J.; Whitmarsh, A. J.; Barrett, T.; Derijard, B.; Davis, R. J. MKK3- and MKK6-regulated gene expression is mediated by the p38 mitogen-activated protein kinase signal transduction pathway. *Mol. Cell. Biol.* **1996**, *16*, 1247–1255. (b) Schieven, G. L. The Biology of p38 kinase: a central role in inflammation. *Curr. Top. Med. Chem.* **2005**, *5*, 921–928.
- (3) (a) Lee, M. R.; Dominguez, C. MAP kinase p38 inhibitors: Clinical results and an intimate look at their interactions with p38 $\alpha$  protein. *Curr. Med. Chem.* **2005**, *12*, 2979–2994. (b) Goldstein, D. M.; Gabriel, T. Pathway to the clinic: Inhibition of p38 MAP kinase. A review of ten chemotypes selected for development. *Curr. Top. Med. Chem.* **2005**, *5*, 1017–1029. (c) Pettus, L. H.; Wurz, R. P. Small molecule p38 MAP kinase inhibitors for the treatment of inflammatory diseases: novel structures and developments during 2006–2008. *Curr. Top. Med. Chem.* **2008**, *8*, 1452–1467. (d) Aston, N. M.; Bamborough, P.; Buckton, J. B.; Edwards, C. D.; Holmes, D. S.; Jones, K. L.; Patel, V. K.; Smees, P. A.; Somers, D. O.; Vitulli, G.; Walker, A. L. p38 $\alpha$  Mitogen-activated protein kinase inhibitors: optimization of a series of biphenylamides to give a molecule suitable for clinical progression. *J. Med. Chem.* **2009**, *52*, 6257–6269. (e) Selness, S. R.; Devraj, R. V.; Monahan, J. B.; Boehm, T. L.; Walker, J. K.; Devadas, B.; Durley, R. C.; Kurumbail, R.; Shieh, H.; Xing, L.; Hepperle, M.; Rucker, P. V.; Jerome, K. D.; Benson, A. G.; Marrufo, L. D.; Madsen, H. M.; Hitchcock, J.; Owen, T. J.; Christie, L.; Promo, M. A.; Hickory, B. S.; Alvira, E.; Naing, W.; Bleviss-Bal, R. Discovery of N-substituted pyridinones as potent and selective inhibitors of p38 kinase. *Bioorg. Med. Chem. Lett.* **2009**, *19*, 5851–5856. (f) Goldstein, D. M.; Kuglstat, A.; Lou, Y.; Soth, M. J. Selective p38 $\alpha$  inhibitors clinically evaluated for the treatment of chronic inflammatory disorders. *J. Med. Chem.* **2010**, *53*, ASAP.
- (4) (a) Herberich, B.; Cao, G.-Q.; Chakrabarti, P. P.; Falsey, J. R.; Pettus, L.; Rzas, R. M.; Reed, A. B.; Reichelt, A.; Sham, K.; Thaman, M.; Wurz, R. P.; Xu, S.; Zhang, D.; Hsieh, F.; Lee, M. R.; Syed, R.; Li, V.; Grosfield, D.; Plant, M. H.; Henkle, B.; Sherman, L.; Middleton, S.; Wong, L. M.; Tasker, A. S. Discovery of highly selective and potent p38 inhibitors based on a phthalazine scaffold. *J. Med. Chem.* **2008**, *51*, 6271–6279. (b) Tasker, A.; Zhang, D.; Cao, G.; Chakrabarti, P.; Falsey, J. R.; Herberich, B. J.; Hungate, R. W.; Pettus, L. H.; Reed, A.; Rzas, R. M.; Sham, K. K. C.; Thaman, M. C.; Xu, S. Preparation of phthalazine, aza- and diaza-phthalazine compounds as protein kinase, especially p38 kinase, inhibitors for treating inflammation and related conditions. PCT Int. Appl. WO 2006094187, 2006.
- (5) Pettus, L. H.; Xu, S.; Cao, G.-Q.; Chakrabarti, P. P.; Rzas, R. M.; Sham, K.; Wurz, R. P.; Zhang, D.; Middleton, S.; Henkle, B.; Plant, M. H.; Saris, C. J. M.; Sherman, L.; Wong, L. M.; Powers, D. A.; Tudor, Y.; Yu, V.; Lee, M. R.; Syed, R.; Hsieh, F.; Tasker, A. S. 3-Amino-7-phthalazinylbenzoxazoles as a novel class of potent, selective, and orally available inhibitors of p38 $\alpha$  mitogen-activated protein kinase. *J. Med. Chem.* **2008**, *51*, 6280–6292.
- (6) (a) Wurz, R. P.; Pettus, L. H.; Xu, S.; Henkle, B.; Sherman, L.; Plant, M.; Miner, K.; McBride, H.; Wong, L. M.; Saris, C. J. M.; Lee, M. R.; Chmait, S.; Mohr, C.; Hsieh, F.; Tasker, A. S. Part 1: Structure-activity relationship (SAR) investigations of fused pyrazoles as potent, selective and orally available inhibitors of p38 $\alpha$  mitogen-activated protein kinase. *Bioorg. Med. Chem. Lett.* **2009**, *19*, 4724–4728. (b) Wurz, R. P.; Pettus, L. H.; Henkle, B.; Sherman, L.; Plant, M.; Miner, K.; McBride, H. J.; Wong, L. M.; Saris, C. J. M.; Lee, M. R.; Chmait, S.; Mohr, C.; Hsieh, F.; Tasker, A. S. Part 2: Structure-activity relationship (SAR) investigations of fused pyrazoles as potent, selective and orally available inhibitors of p38 $\alpha$  mitogen-activated protein kinase. *Bioorg. Med. Chem. Lett.* **2010**, *20*, 1680–1684.
- (7) Pettus, L. H.; Tasker, A.; Xu, S.; Wurz, R. Preparation of pyrazolopyridones as p38 MAP kinase inhibitors which lower plasma concentrations of TNF $\alpha$ , IL-1, IL-6, and/or IL-8. PCT Int. Appl. WO 2008137176, 2008.
- (8) Raitio, K. H.; Savinainen, J. R.; Vepsäläinen, J.; Laitinen, J. T.; Poso, A.; Jaervinen, T.; Nevalainen, T. Synthesis and SAR Studies of 2-Oxoquinoline Derivatives as CB2 Receptor Inverse Agonists. *J. Med. Chem.* **2006**, *49*, 2022–2027.
- (9) For a related halodecarboxylation of lithium carboxylate, see: Chowdhury, S.; Roy, S. The first example of a catalytic hunsdiecker reaction: synthesis of  $\beta$ -halostyrenes. *J. Org. Chem.* **1997**, *62*, 199–200.
- (10) Liu, H.; Ko, S.-B.; Josien, H.; Curran, D. P. Selective N-functionalization of 6-substituted-2-pyridones. *Tetrahedron Lett.* **1995**, *36*, 8917–8920.
- (11) Prepared *in situ* from the palladium-catalyzed reaction of 7-iodo-N,6-dimethylbenzo[d]isoxazol-3-amine and 4,4,5,5-tetramethyl-1,3,2-dioxaborolane, see: (a) Pettus, L. H.; Tasker, A.; Xu, S.; Wurz, R. Preparation of pyrazolopyridones and pyrazolopyrazinones as p38 protein kinase modulators. PCT Int. Appl. WO 2008136948, 2008. (b) Baudoin, O.; Guénard, D.; Guéritte, F. Palladium-catalyzed borylation of ortho-substituted phenyl halides and application to the one-pot synthesis of 2,2'-disubstituted biphenyls. *J. Org. Chem.* **2000**, *65*, 9268–9271.
- (12) Haar, E. Activating MAPKAP kinase 2. *Structure* **2003**, *11*, 611–612.
- (13) HepG2 cells were transfected with a luciferase reporter construct driven by CYP3A4 gene and human PXR cDNA. Cells were exposed to test article and the luciferase activity was determined by chemiluminescence and reported as a percentage of positive control using Rifampin (10  $\mu$ M). Compounds were administered from DMSO stocks to achieve a final concentration of 2 and 10  $\mu$ M in a buffer solution. The incubation duration was 24 h. When tested at 2 and 10  $\mu$ M, **3g** had hPXR activity of 12% and 18% of positive control, while **3d** had 5% and 10% of positive control.
- (14) PDB# 3LHJ.
- (15) For references comparing DFG-in and DFG-out binding, see: (a) Nagar, B.; Bornmann, W. G.; Pellicena, P.; Schindler, T.; Veach, D. R.; Miller, W. T.; Clarkson, B.; Kuriyan, J. Crystal structures of the kinase domain of c-Abl in complex with the small molecule inhibitors PD173955 and imatinib (STI-571). *Cancer Res.* **2002**, *62*, 4236–4243. (b) Zuccotto, F.; Ardini, E.; Casale, E.; Angiolini, M. Through the “gatekeeper door”: exploiting the active kinase conformation. *J. Med. Chem.* **2010**, *53*, ASAP.
- (16) Alanine is rare as a floor residue in the ATP binding pocket. Only 7 out of the 518 kinases have alanine as the floor residue. Manning, G.; Whyte, D. B.; Martinez, R.; Hunter, T.; Sudarsanam, S. The protein kinase complement of the human genome. *Science* **2002**, *298*, 1912–1934.
- (17) Binding constant ( $K_d$ ) values were measured by Ambit Bioscience. For more information, see: [http://www.kinomescan.com/pdfs/Sample\\_Kd\\_Report.pdf](http://www.kinomescan.com/pdfs/Sample_Kd_Report.pdf)
- (18) **3j** had a hPXR level of 37% of positive control at 2  $\mu$ M; it was not tested at 10  $\mu$ M. **3m** had hPXR level of 8% and 46% of positive control at 2 and 10  $\mu$ M, respectively.
- (19) Dominguez, C.; Powers, D. A.; Tamayo, N. p38 MAP kinase inhibitors: Many are made, but few are chosen. *Curr. Opin. Drug Discovery Dev.* **2005**, *8*, 421–430.
- (20) Physicochemical properties were calculated using the Daylight Toolkit, within Amgen's proprietary software (ADAAPT). For more information, see: (a) Daylight Chemical Information Systems, Inc. <http://www.daylight.com>. (b) Cho, S. J.; Sun, X.; Harte, W. ADAAPT: Amgen's data access, analysis, and prediction tools. *J. Comput.-Aided Mol. Des.* **2006**, *20*, 249–261.
- (21) For more information, see: <http://www.ambitbio.com/technology>
- (22) (a) Goldstein, D. M.; Alfredson, T.; Bertrand, J.; Browner, M. F.; Clifford, K.; Dalrymple, S. A.; Dunn, J.; Freire-Moar, J.; Harris, S.; Labadie, S. S.; La Fargue, J.; Lapierre, J. M.; Larrabee, S.; Li, F.; Papp, E.; McWeeney, D.; Ramesha, C.; Roberts, R.; Rotstein, D.; San Pablo, B.; Sjogren, E. B.; So, O.-Y.; Talamas, F. X.; Tao, W.; Trejo, A.; Villasenor, A.; Welch, M.; Welch, T.; Weller, P.; Whiteley, P. E.; Young, K.; Zipfel, S. Discovery of N-[5-Amino-1-(4-fluorophenyl)-1H-pyrazol-4-yl]-[3-(2,3-dihydroxypropoxy)-phenyl]methanone (RO3201195), an orally bioavailable and highly selective inhibitor of p38 map kinase. *J. Med. Chem.* **2006**, *49*, 1562–1575. (b) Liu, C.; Wroblewski, S. T.; Lin, J.; Ahmed, G.; Metzger, A.; Wityak, J.; Gillooly, K. M.; Shuster, D. J.; McIntyre, K. W.; Pitt, S.; Shen, D. R.; Zhang, R. F.; Zhang, H.; Doweiko, A. M.; Diller, D.; Henderson, I.; Barrish, J. C.; Dodd, J. H.; Schieven, G. L.; Leftheris, K. 5-Cyanopyrimidine derivatives as a novel class of potent, selective, and orally active inhibitors of p38 $\alpha$  MAP kinase. *J. Med. Chem.* **2005**, *48*, 6261–6270.
- (23) CYP450 inhibition was measured using human liver microsomes.
- (24) CYP450 induction was measured using fresh human hepatocytes.
- (25) (a) Perretti, M.; Duncan, G. S.; Flower, R. J.; Peers, S. H. Serum corticosterone, interleukin-1 and tumor necrosis factor in rat experimental endotoxemia: Comparison between Lewis and Wistar strains. *Br. J. Pharmacol.* **1993**, *110*, 868–874. (b) Trentham, D. E.; Townes, A. S.; Kang, A. H. Autoimmunity to type II collagen: an experimental model of arthritis. *J. Exp. Med.* **1977**, *146*, 857–868.